MASTERARBEIT / MASTER'S THESIS

Titel der Masterarbeit / Title of the Master's Thesis

"The Fornberg Whitham equation, modelling and some numerical experiments"

verfasst von / submitted by

Michael Fischer, BSc

angestrebter akademischer Grad / in partial fulfilment of the requirements for the degree of

Master of Science (MSc)

Wien, 2018 / Vienna, 2018

Studienkennzahl lt. Studienblatt / degree programme code as it appears on the student record sheet:	A 066 821
Studienrichtung lt. Studienblatt / degree programme as it appears on the student record sheet:	Masterstudium Mathematik
Betreut von / Supervisor:	ao. Univ.-Prof. Mag. Dr. Günther Hörmann

Inhaltsverzeichnis

Abstract

We analyse the nonlinear Fornberg Whitham equation

$$\begin{aligned} u_t + uu_x + v &= 0 \\ v - v_{xx} &= u_x \end{aligned}$$

which describes dispersive waves. We numerically answer open questions from [8]. We use the Godunov method for the hyperbolic part of the equation. This and other analytical and numerical basics of hyperbolic conservation laws are introduced in detail beforehand. A connection is provided for the similarity of the Fornberg Whitham and Burgers equation depending on the initial data.

Abstract

Wir analysieren die nicht-lineare Fornberg Whitham Gleichung

$$\begin{aligned} u_t + uu_x + v &= 0 \\ v - v_{xx} &= u_x \end{aligned}$$

welche dispersive Wellen beschreibt. Mit nummerischen Methoden beantworten wir offene Fragen aus [8]. Wir nutzen das Godunov Verfahren für den hyperbolischen Teil der Gleichung. Dieses sowie andere analytische und nummerische Grundlagen werden zuvor eingeführt. Es wird ein Zusammenhang zwischen der Ähnlichkeit der Fornberg Whitham mit der Burgers Gleichung in Abhängigkeit der Startbedingung hergestellt.

Acknowledgement

First of all I would like to thank my supervisor Günther Hörmann. By chance I found this interesting topic through him. My later change of content, more in the direction of applied mathematics, also received his approval.

I would like to thank David, Oliver and Josef who have always had an open ear for my thoughts during the last months.

The biggest thanks go to Julia, who has tirelessly supported me in the last few years, especially in my fatherly duties.

I would like to dedicate this work to my son Isaak, without him this degree would certainly have been faster, but not more beautiful to achieve.

1 Introduction

The Fornberg Witham equation (FWE) is a nonlinear wave equation. It combines both effects of shallow water theory and typical dispersive behaviour. So solitons and wave breaking occur. A soliton is a fixed wave form travelling to the right (or left) with phase speed c maintaining its shape. Mathematically speaking, wave breaking is the transition from a smooth solution to a discontinuous solution with one or multiple jumps.

In our equation u describes the profile of a wave at the point (x, t). One way of representation is given by

$$\begin{aligned} u_{txx} - u_t + 3u_x u_{xx} + u u_{xxx} - u u_x + u_x = 0, \\ u(x,0) = u_0(x), \end{aligned} \tag{1.1}$$

this was first modelled by Witham in 1974. We consider this nonlinear partial differential equation in case of periodic boundary conditions, a situation recently investigated by Hörmann and Okamoto.

In particular we will present numerical results which address questions they raised in [8], section 4. The main topic are boundedness and lifetime of classical solutions depending on the starting condition. In addition, they posed the question of whether travelling waves with more than one jump exist, they excluded the fall for a single jump.

The numerical solver is based on the following reformulation

$$\begin{aligned} u_t + u u_x + v = 0 \\ v - v_{xx} = u_x \end{aligned} \tag{1.2}$$

with $(1 - \partial_x^2)^{-1} u_x = v$. In chapter 3.1, we go into more detail about the various forms of representation.

We start by discussing the analysis of the linear transport equation and the Burgers equation, since we expect a similar behaviour of solutions to (1.1). Hence numerical schemes developed for the transport and Burgers equation will be generalized to (1.2). Thereby we will discuss the Godunov method in detail.

In chapter 3, we model the Fornberg Witham equation and mention shortly their similarities with the Korteweg de Vries-equation. In the following we repeat important analytical results and explain the numerical approach. Then follows an overview of the numerically obtained findings.

Chapter 4 draws a conclusion of our numerical results.

Thankfully Prof. Dr. Ansgar Jüngel provided some of his graphs from his lecture notes *Modeling and Numerical Approximation of Traffic Flow Problems* for the introductory chapters. The remaining drawings were made with Mathematica and Geogebra.

2 Basic numerical and analytical concepts

2.1 Transport and Burgers equation as first analytical examples

We start by discussion the analysis of the linear transport and Burgers equation. Solutions to both of them exhibit a similar behaviour as the ones to equation (1.1). Therefore we will use numerical methods developed for the two equations to consistently resolve the dynamics of the Fornberg Withham equation. For a more detailed presentation of the analytical methodes and numerical schemes we refer to [4], [12], [16] and [14].

2.1.1 Travelling Waves, weak solutions

The simplest equation in the field of hyperbolic partial differential equations is given by the **transport equation**

$$\begin{aligned} u_t + b \cdot u_x &= 0, \text{ in } \mathbb{R} \times (0, \infty) \\ u(x,0) &= u_0(x) \end{aligned} \tag{2.1}$$

with $b \in \mathbb{R}$. Throughout this thesis we will consider one spatial dimension only since the FWE is prosed in one dimension. However many of the presented methods can be generalized to higher space dimension at the cost of readability. We use the usual convention

$$\frac{\partial}{\partial t} u = u_t, \quad \frac{\partial}{\partial x} u = u_x, \quad \frac{\partial^2}{\partial x^2} u = u_{xx}$$

and the like.

Almost every lecture on the partial differential equations starts with (2.1) so we skip its modelling, for more detail, see [4]. Instead we will now have a look at a special case of solutions for $u_t + bu_x = 0$, namely

$$\phi(x,t) = A \cdot \exp(ikx - i\omega t). \tag{2.2}$$

Inserting (2.2) in (2.1) we obtain the relation

$$\omega = bk \tag{2.3}$$

for ω, $k \in \mathbb{R}$. Later we will call this a **dispersion relation**[1] and $c(k) = \frac{\omega}{k}$ the **phase velocity**

[1] Since we will then also define why the solution of the transport equation is not dispersive, we will dispense with the definition at this point.

One can deduce from this, or via the method of characteristics, the following solution

$$u(x,t) = u_0(x - tb). \tag{2.4}$$

We call this type of solution a **travelling wave** and the phase velocity heuristically the speed of our solution. This can be motivated by a cross-section of our function, see figure 2.1.

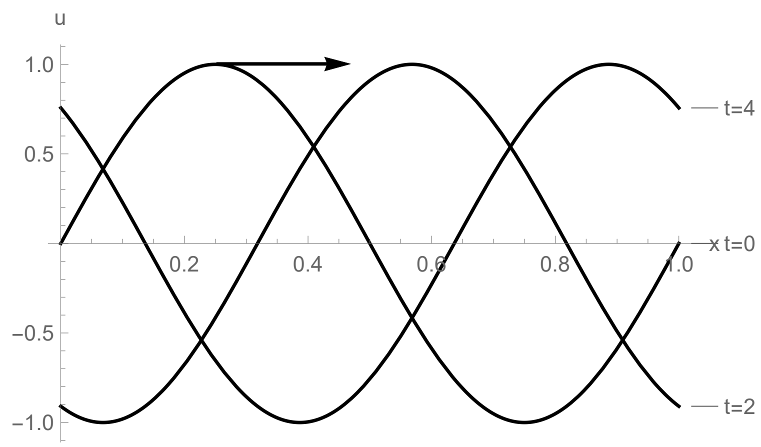

Figure 2.1: Fix e.g. the maximum, then its trajectory in the x,t-plane, colloquial said its speed, is given by $c(k) = b$.

As trivial as the transport equation may be, we will later see that certain typical numerical methods have disadvantages if we apply them to this equation. But more about this later in section (2.2.1).

If one looks at the solution of the equation in [4], [16] or [12], for example, one sees that the **method of characteristics** was used. In [12] it is also motivated that, if u_0 is not C^1, the solution (2.4) is also not C^1, even though, on first view, our equation seems to require this due to the partial derivatives. Therefore we need the concept of weak and distributional solutions. In our case we speak of a **weak solution** u if it satisfies the equation,

$$< L(u), \phi >= 0, \quad \forall \phi \in \mathcal{D}(\mathbb{R})$$

with $L = (\partial_t + b\partial_x)$ and where ϕ is, as usual, an element of the space of **testfunctions** $\mathcal{D}(\mathbb{R})$. We have a short excursus into this area.

2.1.2 $\mathcal{D}$, $\mathcal{D}'$ and H^k

Very often weak solutions are introduced via an integral solution. This makes it very easy to weaken the requirements for solutions in terms of differentiation. With regard to chapter (3.2), however, we briefly introduce the necessary terms of test functions, distributions and Sobolev spaces H^k. The following is based primarily on the lecture notes [12] of Professor Jüngel.

Let Ω be an open subset then we define by

$$\mathcal{D} = C_0^\infty = \{\phi \in C^\infty(\Omega) : \text{supp}(\phi) \text{ is compact in } \Omega\}$$

the space of **testfunctions**. A linear functional $u : \mathcal{D}(\Omega) \to \mathbb{R}$, $\phi \mapsto u(\phi)$ on $\mathcal{D}(\Omega)$ is called **distribution** if and only if it is bounded, that means if for all compact $K \subset \Omega$

$$|u(\phi)| := | < u, \phi > | \leq C\|\phi\|_{C^k(K)}$$

holds, with

$$\|\phi\|_{C^k(K)} := \sum_{|\alpha|\leq k} \sup_{x\in K} |D^\alpha \phi|.$$

The **set of all distributions** is called $\mathcal{D}'$. What does this have to do with integral solutions, derived for example from integration by parts such as in [4] or [**?**, levandosky] The following theorem establishes the connection

Theorem 1 *[12], chapter 3, Lemma 3.4*

Every function $f \in L^1_{loc}(\Omega) = \{f : \Omega \to \mathbb{R}$, measurable : $\forall$ compact $K \subset \Omega$: $f|_K \in L^1(K)\}$ can be seen as a distribution via

$$< f, \phi >:= \int_\Omega f\phi dx \qquad \forall \phi \in \mathcal{D}(\Omega).$$

We then can define weak and distributional solutions. A function u is called **distributional solution** of $L(u) = f$, if $u \in \mathcal{D}'(\Omega)$ and when $L(u) = f$ in the distributional sense, that means $< L(u) - f, \phi >= 0$ for all $\phi \in \mathcal{D}(\Omega)$. A distributional solution is called **weak solution**, if $u \in L^1_{loc}(\Omega)$.

Also very important for us are the so-called Sobolev spaces H^k. These can be characterized as follows.

Theorem 2 *[12], chapter 5, Theorem 5.4*

Let $\Omega \subset \mathbb{R}^n$ be open. Then the set of Sobolev spaces can be characterized as

$$H^k(\Omega) = \{u \in L^2(\Omega) : D^\alpha u \in L^2(\Omega) \text{ for all } |\alpha| \leq k\},$$

where $D^\alpha u \in D'(\Omega)$ is the distributional derivative of u

$$< D^\alpha u, \phi >= (-1)^{|\alpha|} < u, D^\alpha \phi >, \qquad u \in \mathcal{D}'(\Omega), \phi \in \mathcal{D}(\Omega).$$

So now we know about distributional and weak solutions and how, for example, the solution of the transport equation can be defined with discontinuous initial condition. Weak solutions are also used in the investigation of the Burgers equation. Here one usually uses the already mentioned method of characteristics. We recall the main features observed, such as shock formation and rarefraction waves. We will not study the method of characteristics in detail, but for a reader being familiar with the phenomena that arise from intersecting characteristics in the Burgers equation will be helpful. For a simple introduction in applications [13] is sufficient.

2.1.3 Characteristics, Rankine-Hugoniot- and entropy conditions

The (non viscous) Burgers equation is a nonlinear partial differential equation in quasi-linear form, that is

$$\begin{aligned} u_t + uu_x &= 0, \\ u(x,0) &= u_0(x), \end{aligned} \tag{2.5}$$

which can be written as a **conservation law**

$$\begin{aligned} u_t + [f(u)]_x &= 0, \\ u(x,0) &= u_0(x), \end{aligned} \tag{2.6}$$

with $f(u) = \frac{u^2}{2}$. Note that equation (2.1) is conservative if b is constant or divergence free. The function f is the so-called **flow**. In the Burgers equation the characteristics can be specified explicitly via

$$\begin{aligned} x(t) &= f'(u_0(x_0))t + x_0 \\ &= u_0(x_0))t + x_0 \end{aligned} \tag{2.7}$$

We see that the slope of the curves depend on u_0! For the analysis as well as the construction of numerical schemes the corresponding **Riemann problem** is of particular interest. It corresponds to (2.6) with a discontinuous initial condition of the form

$$u_0(x) = \begin{cases} u_l, & x < x_0 \\ u_r, & x \geq x_0. \end{cases}$$

The Burgers equation is not only the simplest equation to introduce and or repeat the above mentioned notions, the solution of the Riemann problem will also play an important role in our numerical procedure later.

Depending on the magnitude of u_l and u_r different phenomena occur. Since the characteristic speed is proportional to u, characteristics intersect if $u_l > u_r$. The so-called velocity of the characteristic can also be recognized heuristically by the already introduced phase velocity c for (2.6). Insert (2.2) in (2.6)

$$-\omega\phi + \phi ik\phi = 0 \tag{2.8}$$

$$c(k) = -\phi \tag{2.9}$$

Figure 2.2 shows the intersecting characteristics. The method of characteristics therefore does not give us a solution, since different characteristics require our solution to meet different conditions[2].

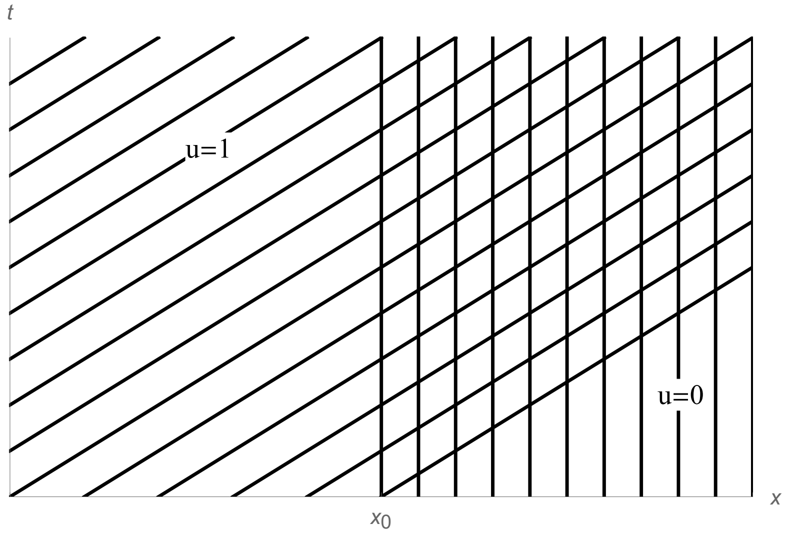

Figure 2.2: The charakteristics interesect, the solution can not be continuous.

To solve this problem, one introduces the **Rankine-Hugoniot jump condition**. Since our solutions do not have to be continuous, jumps/shocks may occur. The Rankine-Hugoniot jump condition now indicates how fast this shock must move. It is defined for each equation individually, for later obvious reasons we do not prove it here for (2.6) but for a more general case, the case of the Burgers equation follows for $g = 0$. Before that we have to define, analogous to the transport equation, what is a weak solution for our Burgers equation. In this case we speak of a weak solution u if it satisfies the equation,

$$< L(u), \phi >= 0, \quad \forall \phi \in \mathcal{D}(\mathbb{R}),$$

with L being the nonlinear differential operator $L : u \mapsto u_t + [f(u)]_x$ or written in the weak formulation

$$\int_0^\infty \int_{-\infty}^\infty u\phi_t + f(u)\phi_x + g(u)\phi dxdt = 0, \quad \forall \phi \in \mathcal{D}(\mathbb{R}),$$

which is used in the following theorem.

Theorem 3 *([4], section 3.4.1.a)*
Let g be a continuous operator in $L^2 \to C \cap L^\infty$ and $f \in C^1(\mathbb{R})$. If u is a integral solution of the equation

$$\begin{aligned} u_t + [f(u)]_x + g(u) = 0 \\ u(x,0) = u_0(x), \end{aligned} \tag{2.10}$$

[2]However, we would like to note that it can be shown that shocks in the Burger equation also can occur with continuous initial conditions.

so that u is discontinuous along the curve $t \mapsto (\Sigma(t), t)$, andotherwise C^1 then u and the curve must fulfil the condition

$$\frac{f(u_l) - f(u_r)}{u_l - u_r} = \sigma(t) := \Sigma'(t) \tag{2.11}$$

where u_l, u_r are the limits from the left- and right-side along Σ.

Proof *As can be found in [4] and [13], a weak solution for (2.10) can be written as*

$$\int_0^\infty \int_{-\infty}^\infty u\phi_t + f(u)\phi_x + g(u)\phi dxdt + \int_{-\infty}^\infty u_0(x)\phi(x,0)dx = 0 \tag{2.12}$$

where ϕ is a suitable test function. In the following, we will shorten a few steps and will only emphasize that $g(u)$ of the above form makes no difference in the proof. For more details we refer to the two mentioned sources. For simplicity let ϕ be a smooth test function such that $\phi(x,0) = 0$ and we break up the first integral into two regions Ω^-, Ω^+ defined via Σ

$$\Omega^- = \{(x,t) : 0 < t < \infty, -\infty < x < \Sigma(t)\}$$
$$\Omega^+ = \{(x,t) : 0 < t < \infty, \Sigma(t) < x < \infty\}.$$

Since $\phi(x,0) = 0$ we can write (2.12) as

$$\int\int_{\Omega^-} u\phi_t + f(u)\phi_x + g(u)\phi dxdt + \int\int_{\Omega^+} u\phi_t + f(u)\phi_x + g(u)\phi dxdt = 0. \tag{2.13}$$

As in [4] we use the Divergence Theorem and the fact, that ϕ has compact support and $\phi(x,0) = 0$ to get for the two integrals in (2.13)

$$\begin{aligned}&\int\int_{\Omega^-} u\phi_t + f(u)\phi_x + g(u)\phi dxdt = \\ &= -\int\int_{\Omega^-} (u_t + [f(u)]_x + g(u))\phi dxdt + \int_{x=\Sigma(t)} [u^-\phi\nu_2 + f(u^-)\phi\nu_1 ds,\end{aligned} \tag{2.14}$$

$$\begin{aligned}&\int\int_{\Omega^+} u\phi_t + f(u)\phi_x + g(u)\phi dxdt = \\ &= -\int\int_{\Omega^-} (u_t + [f(u)]_x + g(u))\phi dxdt - \int_{x=\Sigma(t)} [u^+\phi\nu_2 + f(u^+)\phi\nu_1 ds.\end{aligned} \tag{2.15}$$

Here (ν_1, ν_2) is the outward unit normal to Ω^-. In the next step we remember that

$$u_t + [f(u)]_x + g(u) = 0$$

which shows that the difference of the right hand sides of (2.14) and (2.15) is independent of g. The proof can be finished analogue by using (2.14) and (2.15) in (2.13)

$$\frac{f(u^-) - f(u^+)}{u^- - u^+} = -\frac{\nu_2}{\nu_1}.$$

It remains to observe the fact, that $(1, \Sigma'(t)) \perp -(\nu_2, \nu_1)$ *along* $\Sigma(t)$.

Please note, we have chosen this more general version than in [4]. In [19] there was analyzed the corresponding partial differential equation with $g \in C(\mathbb{R})$ in 1970. However, we would like to point out that our equation (1.2) does not fall into this class of equations because the operator $(1 - \partial_x)^{-1}$ is not defining pointwise a function in $C(\mathbb{R})$ but in our case a bounded operator $L^2 \to C \cap L^\infty$. Hörmann and Okamoto generalized Ǩruzkovs work in Section 2 of [8] for the Fornberg Whitham equation with periodic boundary conditions.

In the following we will always use σ for the **speed of a shock**. Now we can display our solution u as follows, in short only graphically.

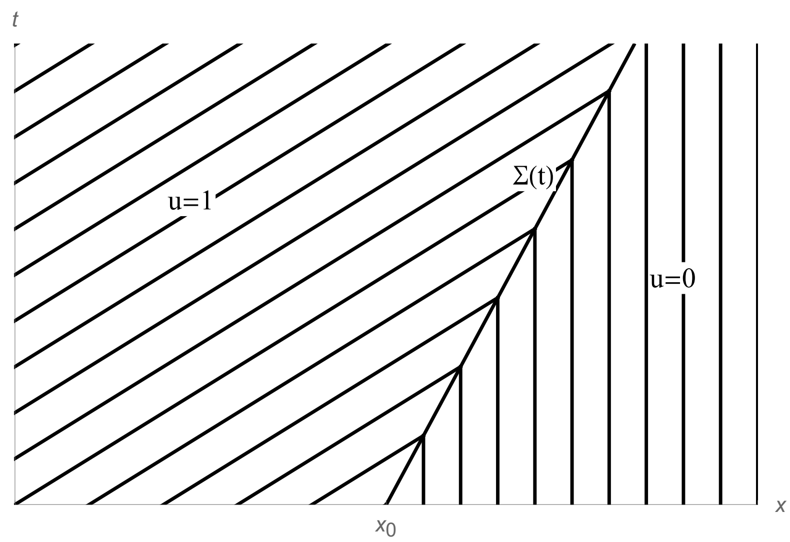

Figure 2.3: The shock Σ starts in x_0.

If u_l is smaller than u_r, a region with void appears as can be seen in figure 2.4

As [4] writes, an intuitive solution is to use the shock condition and continue the left and right solutions constant till Σ. However, as one can show, this is not the only solution and one introduces a so-called **rarefaction wave** as a second solution

The second introduced solution is in C so the question occurs, which solution is the right one and what does "right" means in our context? How do we deal with the loss of uniqueness? We find a way out by introducing a so-called **entropy condition**. Colloquially spoken and known from reality, a larger wave moves faster than a smaller one as we have seen in (2.8). Thus the speed of a solution is directly proportional to u and that

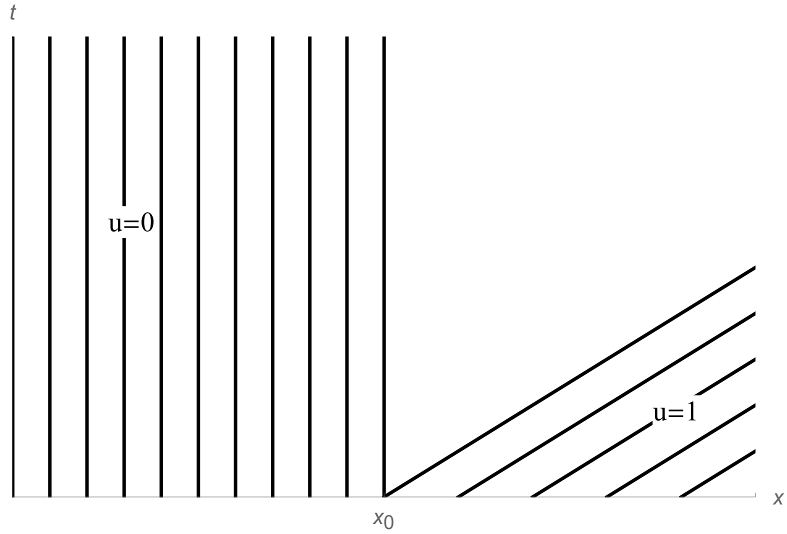

Figure 2.4: The method of charakteristics give us not enough information, here the special case $u_l = 0$.

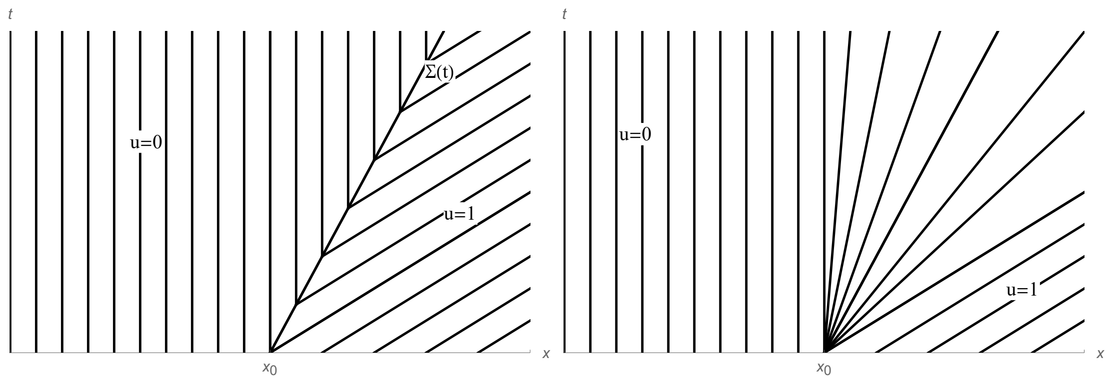

Figure 2.5: On the left the shock solution, on the right, a rarefunction wave starting in x_0 continuously connects the two solutions.

results in waves breaking. In colloquial terms, the tip of the wave moves faster than the bottom and the solution overlaps.

However, this is only the case if u_l to the left of the shock Σ is greater than u_r. Or, in general, if the following applies

$$f'(u_l) > \sigma(t) > f'(u_r). \tag{2.16}$$

This is called the **Lax entropy condition**. With this we can restore uniqueness. We only accept a shock solution if the Lax entropy condition is fulfilled. If we now look again at the two previous cases, we select the shock solution satisfying the Rankine Hugoniot jump condition in the first case since the Lax entropy condition is fulfilled. In the second case, the Lax entropy condition does not hold and thus we choose the rarefaction wave as our solution.

However, it only works for convex flow functions. This can be generalized for non-convex flow functions f with the **Oleinik entropy condition**

$$\frac{f(u_l) - f(u)}{u_l - u} \geq \frac{f(u_l) - f(u_r)}{u_l - u_r} \tag{2.17}$$

for all u between u_l and u_r.

A few remarks:

- Note that for convex f, the Lax and Oleinik entropy condition are equivalent.

- This example often introduces not only the concept of an entropy condition but also a so-called **entropy solution**. To this end the **viscous Burgers equation** is observed,

  $$u_t + [f(u)]_x = \epsilon u_{xx}, \qquad \epsilon > 0.$$

  This equation has a smoothed travelling wave as solution. For $u_l > u_r$ the wave front goes to zero as the diffusion vanishes, that is $\epsilon \to 0$, converging to the expected shock solution. To proof this one needs the terms entropy function and a corresponding entropy flow. We choose the shorter way and are content with the entropy conditions to reach uniqueness. When we later, in the numerical section, point out that our algorithms converge against the entropy solutions, we are satisfied that this means the unique solution which fulfils our entropy condition. Strictly speaking, however, entropy solutions are used in the formulation and proof of the statements.

We conclude by summarizing the results for Burgers equation, for a proof we refer to [4].

Theorem 4 *([4], chapter 3.4.4, Theorem 4)*
Consider the conservation law with Riemann initial conditions

$$u_t + [f(u)]_x = 0 \tag{2.18}$$

$$u_0(x) = \begin{cases} u_l, & x < x_0 \\ u_r, & x \geq x_0. \end{cases} \tag{2.19}$$

If $u_l > u_r$, the unique entropy solution of the Riemann problem (2.23) is

$$u(x,t) := \begin{cases} u_l, & \frac{x-x_0}{t} < \sigma \\ u_r, & \frac{x-x_0}{t} > \sigma \end{cases} \qquad (x \in \mathbb{R}, t > 0)$$

where

$$\sigma = \frac{f(u_l) - f(u_r)}{u_l - u_r}.$$

If $u_l < u_r$, the unique entropy solution of the Riemann problem (2.23) is

$$u(x,t) := \begin{cases} u_l, & \frac{x-x_0}{t} < f'(u_l) \\ (f')^{-1}(\frac{x-x_0}{t}), & f'(u_l) < \frac{x-x_0}{t} < f'(u_r) \\ u_r, & \frac{x-x_0}{t} < f'(u_r) \end{cases} \quad (x \in \mathbb{R}, t > 0)$$

Note that we have slightly generalized the boundary conditions compared to the statement in [4] via the coordinate transformation $x - x_0$. Later it will be important to us that our solution is constant along the line $\frac{x-x_0}{t}$.

2.2 Numerical concepts for transport and Burgers equation

This section is primarily based on [11] and [16], in addition classical literature like [10], [17], [18] and [14] have been included.

2.2.1 Meshs, Centralized-, Lax-Friedrich- and Upwind-schemes

We expect the formation of travelling waves in (1.2) as in the Burgers equation. Hence we will use numerical scheme, which were developed to capture this behaviour correctly. We elaborate those methods on (2.1) and (2.6) with the Riemann problem or periodic boundary conditions as initial data. The construction of these methods is based on the respective Riemann problems and guarantees that the Rankine Hugoniot shock condition and entropy condition are satisfied.

Without limitation of generality we consider the interval $[0,1]$ in our spatial dimension x and a time interval $[0,T]$. When discretizing the domain we stick to a uniform mesh in x and t, that means, we have $x_0 = 0$, $x_N = 1$ and $x_{j+1} - x_j = \Delta x$ for all $j \in \{0, \ldots N-1\}$. We use the same discretization in the t-direction and divide the interval $[0,T]$ into M points $t^n = n\Delta t$ with $n = 0, \ldots, M$. Figure 2.6 shows the space-time grind.

When using periodic initial conditions we will reduce the situation to $u_0(x) = \sin(2\pi x)$. When using non continuous initial conditions we will reduce ourself to the Riemann problem. The classical approach when solving a partial differential equation numerically is to replace the differential quotients with difference quotients by Taylor's expansion. Thus, usually, the time derivative is replaced by a forward difference and the spatial derivative is often replaced by a **centered difference scheme**, that is

$$u_t \approx \frac{u_j^{n+1} - u_j^n}{\Delta t}, \quad u_x \approx \frac{u_{j+1}^n - u_{j-1}^n}{2\Delta x}, \quad j = 0, 1, \ldots, N-1, n = 0, 1, \ldots, M$$

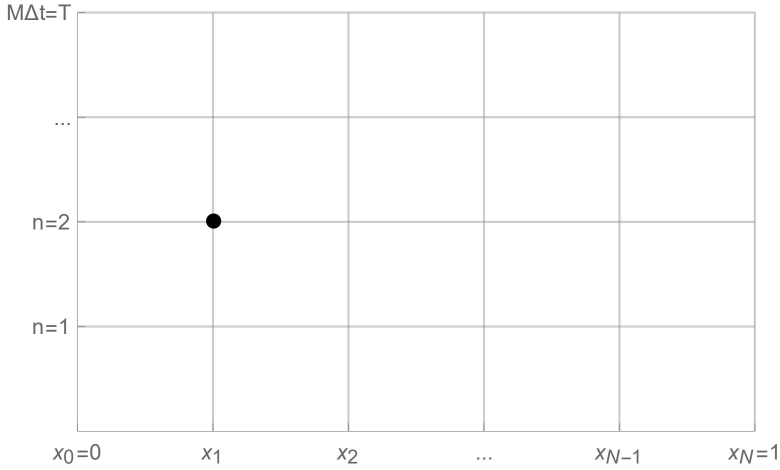

Figure 2.6: Grid with $x_1^2 = (\Delta x, 2\Delta t)$ marked in.

where u_j^n is the approximation of $u(j\Delta x, n\Delta t)$. Our transport equation then reads

$$\frac{u_j^{n+1} - u_j^n}{\Delta t} + b\frac{u_{j-1}^n - u_{j+t}^n}{2\Delta x} = 0, \tag{2.20}$$

$$\Rightarrow u_j^{n+1} = u_j^n - b\frac{\Delta t}{2\Delta x}(u_{j+1}^n - u_{j-1}^n). \tag{2.21}$$

$$\tag{2.22}$$

This is an **explicit scheme** in u_j^{n+1}. As odiscussed in [11] and [16], using the centered difference scheme is unsuitable for conservation laws since the solution oscillates strongly as you can see in figure 2.7.

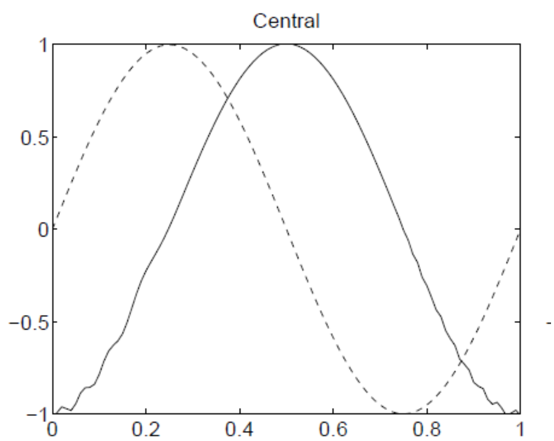

Figure 2.7: We have strong oszilations in our numerical solution, taken from [11].

An a priori justification is the following: The exact solution is a travelling wave.It moves from the left to the right since $b > 0$. However (2.20) uses a central difference quotient and thus uses the information to the left and the right. Therefore it is neglecting the physical property of the equation.

A detailed discussion and analysis of the observed instabilities can be found in [16], page 11.

To improve this oscillation one often uses the **Lax-Friedrichs scheme** in time t, which uses an arithmetic average in its approximation

$$u_j^{n+1} = \frac{1}{2}(u_{j+1}^n - u_{j-1}^n) - b\frac{\Delta t}{2\Delta h}(u_{j+1}^n + u_{j-1}^n)).$$

But then we run into another problem since the numerical solution smears out as can be seen in figure (2.8)

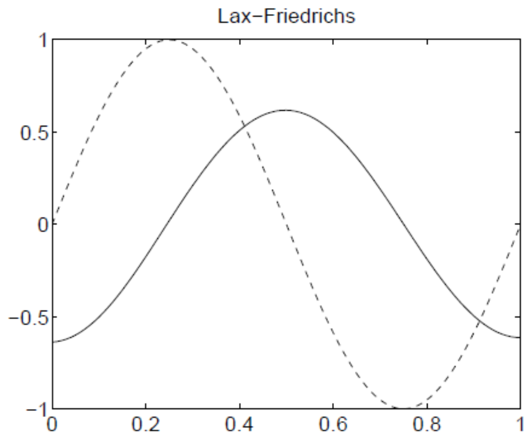

Figure 2.8: Lax-Friedrich brings in artificial diffusion, taken from [11].

[11] shows that the Lax Friedrich flux adds an artificial viscosity term u_{xx}, which is not present in the original equation. The solution of our problem is the so-called **upwind scheme** The motivation for this again is physical. Since the travelling wave moves to the right we compute the discrete derivatives which uses the information from the direction where it comes from:

$$u_t \approx \frac{u_j^{n+1} - u_j^n}{\Delta t}, \quad u_x \approx \frac{u_j^n - u_{j-1}^n}{\Delta x}$$

and thus the upwind scheme reads

$$u_j^{n+1} = u_j^n - b\frac{\Delta t}{\Delta x}(u_j^n - u_{j-1}^n), \quad b > 0.$$

As you can see in figure (2.9), this method shows the correct solution without oscillations but still with artificial diffusion. However, this is much smaller than in the Lax Friedrich method. If we now choose Δt smaller, there seems to be hardly any diffusion

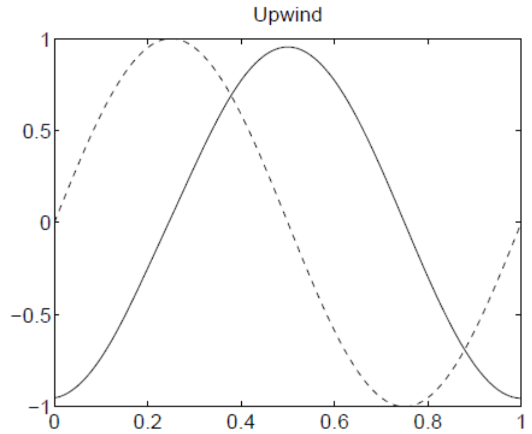

Figure 2.9: Upwind has less artificial diffusion, taken from [11].

and we get almost the exact solution as can be seen in figure (2.10)

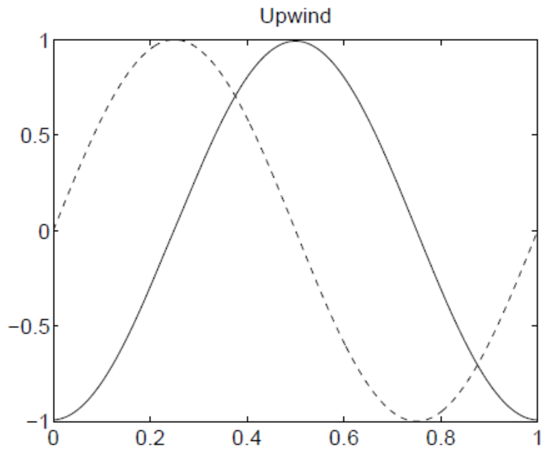

Figure 2.10: Almost no diffusion for the upwind scheme for small Δx, taken from [11].

We would like to note at this point that we can use an analogous **downwind scheme** for $b < 0$ and this concept will be important in our Godunov scheme introduced later .

2.2.2 CFL condition

The smaller the time steps Δt the more iterations are required to determine the solution at a fixed time T. Therefore, the question arises whether we can choose a Δx larger in order to save computational work. Picture (2.11) should answer the question for us intuitively with No.

A short analysis shows that this is due to the so-called **Courant-Friedrich-Levy**

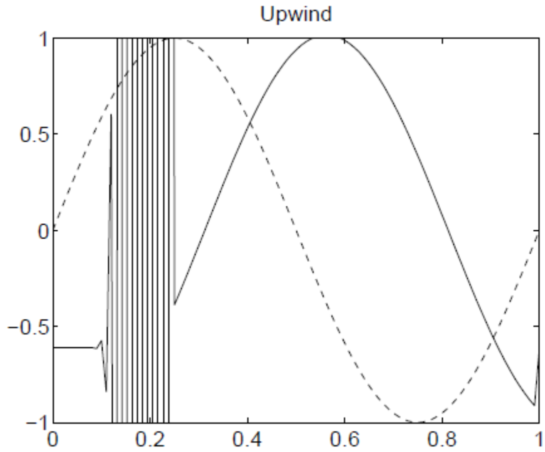

Figure 2.11: The function is oscillating heavily, taken from [11].

(CFL) condition,

$$\frac{|b| \cdot \Delta t}{\Delta x} \leq C$$

where C is the **Courant number**. Since we use an explicit procedure, as usual in conservation equations [11], $C < 1$ must apply so that the explicit algorithm is stable. Not going into detail, we would like to mention that [11] shows how this condition can be derived from artificial diffusion when using the upwind scheme in solving the transport equation.

If we now solve the transport equation with slightly changed Riemann conditions,

$$u_0(x) = \begin{cases} 1, & 0 < x < \frac{1}{2} \\ 0, & \frac{1}{2} \leq x \leq 1. \end{cases} \tag{2.23}$$

while using the upwind scheme, we see in [11] that if we use a high resolution, we approximate the solution well as can be seen in figure (2.12).

2.2.3 Upwind scheme and the conservative formulation of the Burgers equation

If we solve the Burgers equation (2.6) with analogously changed Riemann conditions (2.23), and use the respective upwind formulation

$$u_j^{n+1} = u_j^n - \frac{\Delta t}{\Delta x} u_j^n (u_j^n - u_{j-1}^n)$$

this yields $u_j^0 = 0$ for all $j \geq \frac{N}{2}$ as shown in [11]. Additionally we have $(u_j^0 - u_{j-1}^0) = 1 - 1 = 0$ for all $j < \frac{N}{2}$. This continues in every time step and our numerical solution is $u_j^n = u_j^0$ which means $u(x,t) = u_0(x)$.

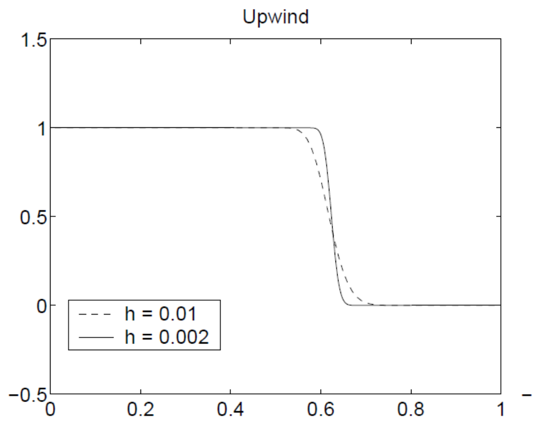

Figure 2.12: The upwind scheme for different $h = \Delta x$, taken from [11].

An obvious idea is that we should better approximate u in $u \cdot u_x$ by u_{j-1}^n and thus use

$$u_j^{n+1} = u_j^n - \frac{\Delta t}{\Delta x} u_{j-1}^n (u_j^n - u_{j-1}^n).$$

But as we see in [11], figure (2.13) that although we receive a shock as a solution, it moves at the wrong speed!

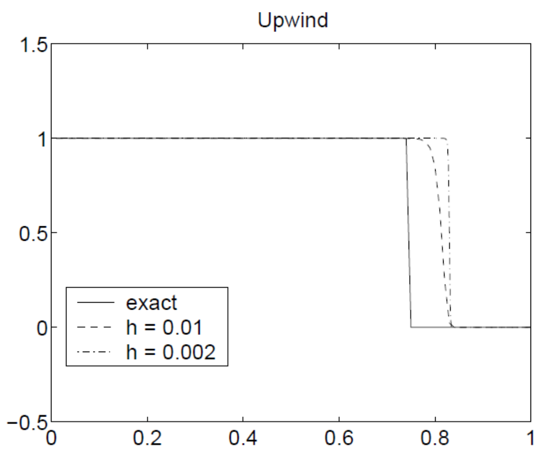

Figure 2.13: The upwind scheme for different $h = \Delta x$, taken from [11].

The problem is that we discretize the equation in quasilinear form. The two different formulations (2.5) and (2.6) are only equivalent for u being at least C^1. Thus we have to consider Burgers equation in conservative form, that was

$$u_t + [f(u)]_x = 0.$$

Thus we get **schemes in conservation form**, that means

$$u_j^{n+1} = u_j^n - \frac{\Delta t}{\Delta x}(F(u_j^n, u_{j+1}^n) - F(u_{j-1}^n, u_j^n)). \tag{2.24}$$

where F is the so-called numerical flux. We would like to note that F is generally a function of several points $u_{j-p}^n, \ldots u_{j+q}^n$, but we restrict our investigation to the above, easiest case. On the other hand, this case immediately leads to a geometric interpretation as a finite volume scheme.

2.2.4 Finite volume scheme and the method of Godunov

In case of the linear transport equation (2.1) the charakteristics are straight lines with equal slope. The direction in which information is transported is known beforehand. Thus we knew when to use the upwind or downwind scheme. In Burgers equation (2.6) this is not the case, because the charakteristic curves depend on u or in other words, in terms of wave analysis, the phase velocity can change its direction depending on u.

The finite volume method (FVM) allows us to discretize convervation laws consistently. We introduce the basic ideas in the following. The FVM is based on the approximation of **cell averages** u_j^n. For this we first need a different view of our mesh, see figure (2.14)

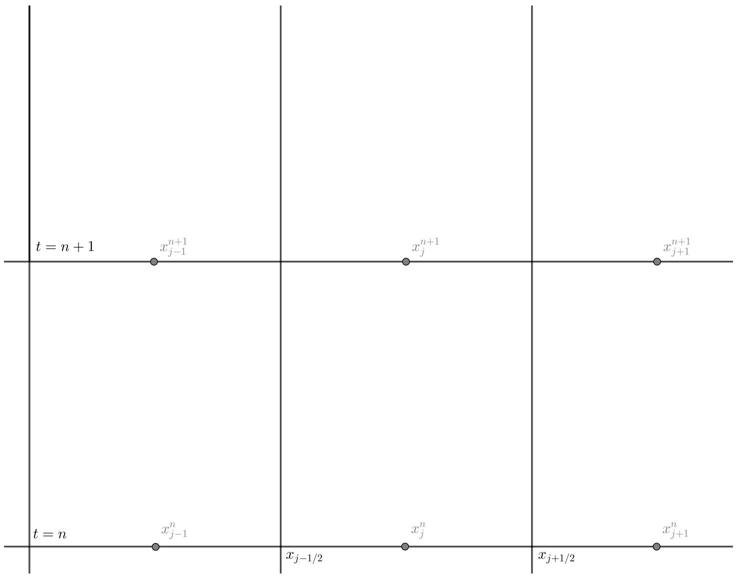

Figure 2.14: Our new finite volume grid, with our previous grid points in grey.

where we define $x_{(j\pm\frac{1}{2})\Delta x}$ with $x_{j\pm\frac{1}{2}}$ and set

$$u_j^n \approx \frac{1}{\Delta x}\int_{x_{j-\frac{1}{2}}}^{x_{j+\frac{1}{2}}} u(x, t^n)dx \tag{2.25}$$

as the cell average at time step t^n. This is well defined for any integrable function, hence also for our weak solutions. How do we obtain then u_j^{n+1}? We integrate our conservation law

$$u_t + (f(u))_x = 0$$

over the domain $[x_{j-\frac{1}{2}}, x_{j+\frac{1}{2}}) \times [t^n, t^{n+1})$ and using heuristically the fundamental theorem of calculus (which only holds for absolute continuous functions in general). This results in

$$\int_{x_{j-\frac{1}{2}}}^{x_{j+\frac{1}{2}}} u(x, t^{n+1})dx =$$
$$= \int_{x_{j-\frac{1}{2}}}^{x_{j+\frac{1}{2}}} u(x, t^n)dx - \int_{t^n}^{t^{n+1}} f(u(x_{j+\frac{1}{2}}, t))dt + \int_{t^n}^{t^{n+1}} f(u(x_{j-\frac{1}{2}}, t))dt.$$

Now we divide by Δx and consider $F(u_j^n, u_j^{n+1})$ as a good approximation of the average flow along $x_{j+\frac{1}{2}}$ over the time interval (t_n, t_{n+1}).

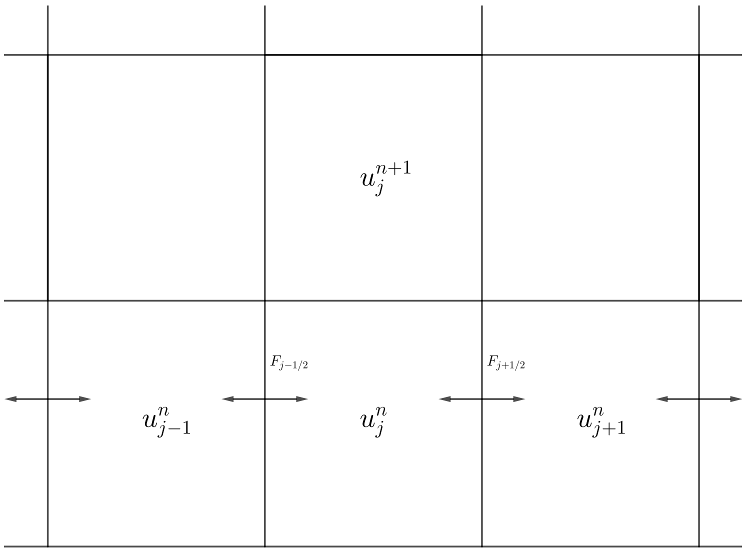

Figure 2.15: Our finite volume grid, here u_j^n are cell averages and F_j^n our fluxes.

Thus we set

$$F(u_j^n, u_{j+1}^n) \approx \frac{1}{\Delta t} \int_{t^n}^{t^{n+1}} f(u(x_{j+\frac{1}{2}}, t))dt.$$

From this we obtain the form (2.24). Now we want to calculate the **numerical flow**

function F for each cell interface $x_{j+\frac{1}{2}}$. The function u is constant along the line $x_{j+\frac{1}{2}}$ (remember the remarks for theorem (4)) for $t^n \leq t \leq t^{n+1}$ depending only on u_j^n and u_{j+1}^n, we denote this value by $u^\star(u_j^n, u_{j+1}^n)$. Then the numerical flux reduces to

$$F(u_j^n, u_{j+1}^n) = f(u^\star(u_j^n, u_{+1}^n)). \tag{2.26}$$

In the case of a convex f we now have to distinguish four cases, as [11][3] and [16] show:

1. If $f'(u_j), f'(u_{j+1}) \geq 0$, then $u^\star = u_j$. A rarefraction wave or a shock, wandering to the right, starts, and upwind is used.

2. If $f'(u_j), f'(u_{j+1}) \leq 0$, then $u^\star = u_{j+1}$. A rarefraction wave or a shock, wandering to the left, starts, and downwind is used.

3. If $f'(u_j) \geq 0 \geq f'(u_{j+1})$, then $u^\star = u_j$ if $\sigma > 0$ or $u^\star = u_{j+1}$ if $\sigma < 0$ where σ is the speed of our shock curve and defined as in theorem 2.11. In the first case, a shock is starting, wandering to the right and upwind is used. In the second case, analogously, a shock is starting, wandering to the left and downwind is used.

4. If $f'(u_j) < 0 < f'(u_{j+1})$, then $u^\star = u_s$, a **transonic rarefaction wave** starts.

Here the value u_s is the solution of $f'(u^\star) = 0$, since f is supposed to be convex, it is unique. In our case, we have $u_s = 0$. The rarefaction wave is called **transonic** and $u^\star$ is called a sonic **point**.

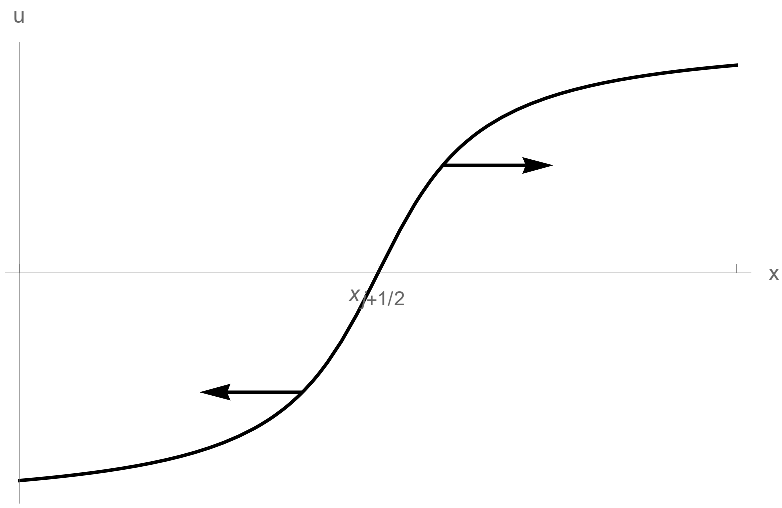

Figure 2.16: Due to the different signs of u, the upper part is moving to the right and the other to the left.

[3]It should be briefly noted here that the author has a small error in his first (and analogue in his second) case, it can be a rarefraction wave or a shock where he states only the first one. But in both cases we get the same result $u^\star = u_j$.

In our case with $f(u) = \frac{u^2}{2}$, we get $f'(u_j) = u_j$ and we can simplify the algorithm even more in the following section.

We still have to rule out one possible problem. The starting rarefaction waves and shocks could meet, so our function would no longer be constant along the lines $x_{j+\frac{1}{2}}$. But this problem can be solved easily. We know the speed of the shock waves, it is fixed by the Rankine Hugoniot condition and the speed of a rarefaction wave, it is given by theorem 4. With a suitably chosen CFL-condition

$$|\frac{\Delta t}{\Delta x} f'(u_j^n)| \leq \frac{1}{2},$$

we manage to avoid the intersection of waves and shocks.

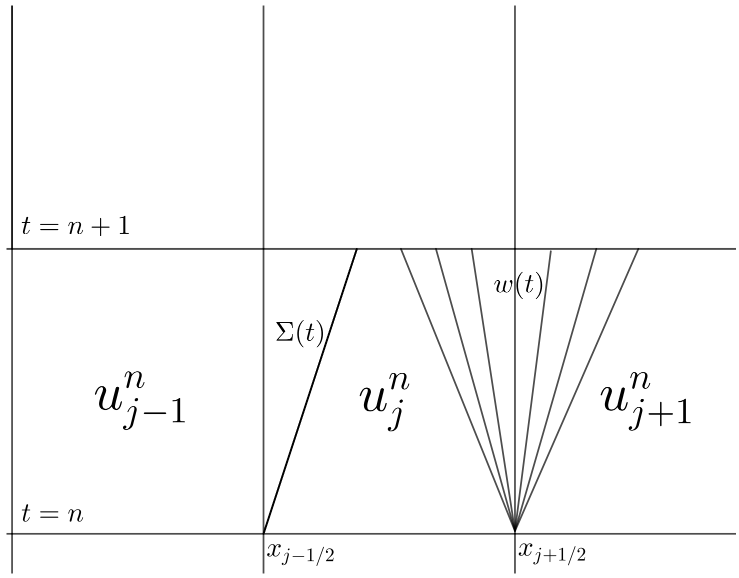

Figure 2.17: If the CFL-condition is met, the shock $\Sigma(t)$ and the rarefunction wave $w(t)$ cannot intersect.

This can be improved. Intersections are allowed if the interaction only happens in one cell. So we can enhance our CFL-condition to

$$|\frac{\Delta t}{\Delta x} f'(u_j^n)| = |\frac{\Delta t}{\Delta x} u_j^n| \leq 1.$$

2.2.5 The Godunov scheme in the Burgers equation

As mentioned, we are now simplifying the algorithm heavily. If we consider the third case, the following holds

$$u_j \geq 0 \geq u_{j+1}.$$

Now the sign of σ decides whether we select the left or the right value. Since our function is convex, it is decided by f being the maximum at those two values.

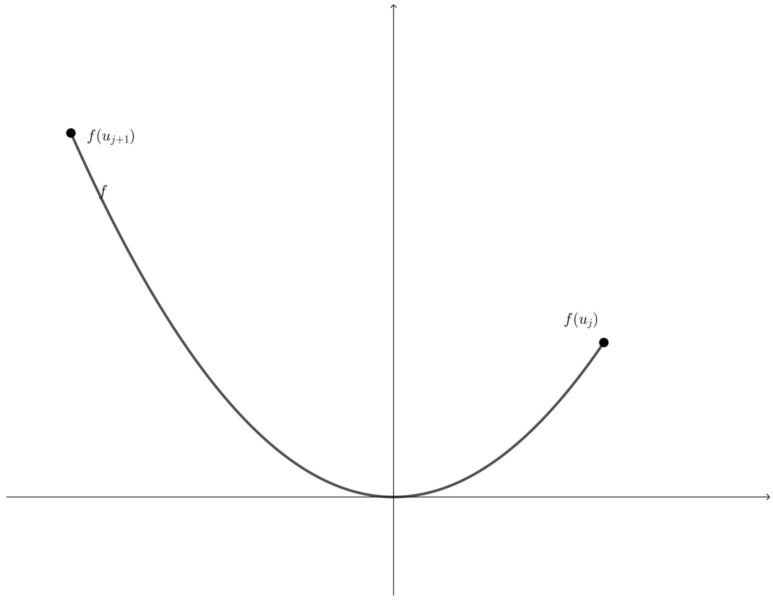

Figure 2.18: With f being convex, the maximum will be at u_j or u_{j+1}.

If this consideration is carried out in all four cases, the following is obtained

$$F(u_j^n, u_{j+1}^n) = \begin{cases} \min_{u_j \leq u \leq u_{j+1}} f(u), & u_j \leq u_{j+1} \\ \max_{u_{j+1} \leq u \leq u_j} f(u), & u_j > u_{j+1} \end{cases}. \tag{2.27}$$

2.2.6 Convergence results

The following section mainly summarizes the results of the work of [2]. Comparable results can be found in classical books like [14], [17] and [10]. We briefly discuss the convergence of the numerical solution to the desired entropy solution. First we state the necessary definition of consistency and monotonicity of a numerical scheme. We call a conservative scheme (2.24) **consistent**, if the numerical flux F is Lipschitz continuous and

$$F(u, u) = f(u) \quad \forall u \in \mathbb{R}.$$

We call a scheme **monotone**, if for given two initial conditions u_0, v_0,

$$\begin{aligned} u_0 &\geq v_0 \\ \Rightarrow u_j^n &\geq v_j^n \end{aligned}$$

holds for all j, n. It can be shown that a scheme written in the form

$$u_j^{n+1} = G(u_{j-p}^n, \dots, u_{j+p}^n) \tag{2.28}$$

is monotone, if and only if G is an increasing function in all of its arguments. And as we know from (2.24), the Godunov scheme can be written like this

$$u_j^{n+1} = G(u_{j-1}^n, u_j^n, u_{j+1}^n).$$

To show that the Godunov method is monotone is not arithmetically difficult, but obviously we have many case distinctions ahead of us. Crandall and Majda avoid this, in a short sketch, but refer to many previous papers and an alternative presentation of the solution. [20] makes this distinction, but also has to introduce a new notation to get the different cases under control. We therefore do not prove the following lemma, for a proof we refer to the above mentioned works. Instead, we then at least show in one case that the Godunov scheme is monotone:

$$0 < u_{j-1}^n < u_j^n < u_{j+1}^n.$$

Then we have

$$G(u_{j-1}^n, u_j^n, u_{j+1}^n) = u_j^n - \frac{\Delta t}{\Delta x}\frac{(u_j^n)^2}{2} + \frac{\Delta t}{\Delta x}\frac{(u_{j-1}^n)^2}{2}$$

In our case, G is constant in the third argument and since $0 < u_{j-1}^n$ is assumed, monotone increasing in the first one. For the second argument define

$$g(u_j^n) := u_j^n - \frac{\Delta t}{\Delta x}\frac{(u_j^n)^2}{2} = u_j^n(1 - \frac{\Delta t}{\Delta x}\frac{(u_j^n)}{2}).$$

The function g is increasing since our CFL condition ensures $|\frac{\Delta t}{\Delta x}u_j^n| \leq 1$ and thus

$$g'(u_j^n) = 1 - \frac{\Delta t}{\Delta x}u_j^n \geq 0.$$

Similar arguments can be used in all other cases, hence we have:

Lemma 1 *The Godunov scheme is a monotone scheme.*

Additionally we need the trivial fact that the Godunov scheme is consistent. The numerical flux F is also Lipschitz since it uses f on a bounded interval. Crandall and Majda showed then in [2]:

Theorem 5 *(Monotone Difference Approximations for Scalar Conservation Laws, Crandall and Majda, 1980)*

Suppose $u_0 \in L^1(\mathbb{R}) \cap L^\infty(\mathbb{R})$ and $a \leq u_0 \leq b$ almost everywhere. Let (2.28) be a consistent conservation-form difference approximation to the scalar conservation law (2.6) which is monotone on $[a, b]$ and which has a Lipschitz continous numerical flux f.

Let $u^{\Delta t}$ be the numerical solution and u be the exact solution of (2.6). We fix the CFL-condition and, as $\Delta t \to 0$, $u^{\Delta t}$ converges to u in $L^1(\mathbb{R})$ uniformly for bounded $t \geq 0$, more precisely

$$\lim_{\Delta t \to 0} \sup_{0 \leq t \leq T} \int_{\mathbb{R}} |u^{\Delta t}(x,t) - u(x,t)| dx = 0.$$

For a detailed proof of the general theorem, see [2].

3 The Fornberg-Whitham equation

3.1 Derivation of the Fornberg-Whitham equation

Both our example equations, transport and Burgers equation have travelling waves as solutions, the latter only in the form of shock formations. As mentioned above, they belong to the class of hyperbolic wave equations. The prototype example therefore is usually the wave equation $u_{tt} = c_0 u_{xx}$, but the simplest example is our transport equation. Due to the non-linearity, shocks also occur for continuous initial data in the Burgers equation. We now want to combine these properties with those of dispersive waves. This is done via the Fornberg-Whitham equation which will be derived below.

Dispersive Waves

Unlike hyperbolic wave equations, dispersive wave equations are often not named by the equation, but by the existence of elementary solutions of the form

$$\phi(x,t) = A \cdot \exp(ikx - i\omega t) \tag{3.1}$$

which we call **sinusoidal wavetrains**. Here[1] k corresponds to the so-called **wave number**, ω the **frequency** and A the **amplitude**.The parameters k and ω are related by

$$\omega = W(k), \tag{3.2}$$

also known as the **dispersion relation**. We recall that these concepts can be generalized to higher space dimensions. We call the quantity

$$\Omega = kx - \omega t$$

the **phase** and we also introduce the general case of the **phase velocity** c by

$$c = \frac{\omega}{k}.$$

For W linear, this is exactly the same as our previously introduced phase velocity.

In order to exclude non-dispersive wave equations which occur for the transport equation and the wave equation, we make the following assumption on our partial differential equation. An partial differential equation is called a **dispersive** wave equation, if it has solutions of the form (3.1) and in addition $W(k)$ is real and $W'' \neq 0$ holds. We then call the solutions **dispersive waves**. Please note that c is also real in this case.

[1] In general, k is a vector representating the direction of the propagating wave ϕ

Whitham generalised the classical theory (in one dimension) of the linear equation with constant coefficients in 1967 using an integrodifferential equation

$$u_t + \int_{-\infty}^{\infty} K(x-s)\partial_s u(s)ds = 0, \tag{3.3}$$

which can be written as $u_t + K * u_x = 0$.

Where does this approach come from? Let us start as an example with the (normalized and) linearised Korteweg-de Vries (KDV) equation,

$$u_t + c_0 u_x + u_{xxx} = 0 \tag{3.4}$$

with c_0 being an adjustable parameter. The KDV equation was first proposed in 1895 by Korteweg and de Vries to describe shallow water waves in narrow channels. It contains soliton solutions, first observed by Russel in 1834. It it shown for example in [3] that it has sinusoidal wavetrains as solutions.

Note that the lhs of (3.4) can be written as $u_t + K_{KDV} * u_x$ ([21]) with $K_{KDV}(x) = c_0\delta(x) + \delta_{xx}(x)$, whereas δ denotes the Delta Dirac. In general K can be an arbitrary sum of δ-distributions and its derivatives to construct any desired dispersion function W.

One step back, in the modelling of an equation as explained in [22] and [3] we usually start with the phase velocity c. As we will see immediately, there is a direct relationship between K and c and we will be able to construct our K for desired c. From this we then obtain our desired differential equation.

If we insert (2.2) ϕ in 3.3, we get

$$-i\omega \exp(ikx) + \int_{-\infty}^{\infty} K(x-s)ik \exp(iks)ds = 0.$$

Now we want to rewrite this equation as a phase velocity c. After dividing by $ik\exp(ikx)$ and using a change of variables inside the integral we obtain

$$c = \frac{\omega}{k} = \int_{-\infty}^{\infty} K(s)\exp(-iks)ds.$$

The right-hand side is the Fourier transformation $\mathcal{F}(K)$ of the kernel K and thus, using the inversion theorem, we can construct K for any desired c, assuming for instance $c, K \in L^1 \cap L^2(\mathbb{R})$

$$K(x) = \frac{1}{2\pi}\int_{-\infty}^{\infty} c(k)\exp(ikx)dk.$$

Thus the velocity $c(k) = c_0 - k^2$ yielded to K_{KDV}. From our definition of dispersive waves, we demanded that c be a real function. Likewise, K should be a real function, which we infer from our real equation (3.3). Therefore, c and K must be even, real functions[2].

Let us now consider a phase velocity $c(k)$ of the form

$$c(k) = c_0 + c_2 k^2 + \dots c_{2m} k^{2m}.$$

Then we obtain

$$K(x) = c_0 \delta - c_2 \delta'' + \dots + (-1)^m c_{2m} \delta^{(2m)},$$

and therefore (3.3) reads as

$$u_t + c_0 u_x - c_2 u_{xxx} + \dots + (-1)^m c_{2m} \frac{\partial^{2m+1} u}{\partial x^{2m+1}} = 0$$

If we replace c by a more general function with an infinite (even) Taylor series (in k) we obtain a differential equation with an infinite series of derivatives, which we again can write as $K * u_x$. This motivated our original equation (3.3).

Whitham now combines via the non-linear part the hyperbolic effects of the Burgers equation with this new idea to get a new class of equations given by

$$u_t + u u_x + K * u_x = 0.$$

For $K = \delta''$ we get the (non-linearised) Korteweg-de Vries equation[3]

$$u_t + u u_x + u_{xxx} = 0.$$

As [3] writes, the Korteweg-de Vries equation has periodic and solitary waves which do not occur in shallow water theory, but there are no typical effects from that theory like shocks occurring in Burgers equation. As can be found in [3] and [6], the linear term u_{xxx} is too strong and thus prevents shocks and wave breaking from occurring.

Therefore we have to modify the velocity c and thus the integral core K to get the desired phenomena.

The Fornberg Whitham equation

In 1978 Fornberg and Whitham suggested

$$c(k) = \frac{1}{1+k^2}, \quad K(x) = \frac{1}{2}\exp(-x),$$

[2]This follows from the fact that the Fourier transform of the odd part of a real function is imaginary which is neither K nor c ([23]).

[3]In most cases the term $6uu_x$ can be found in the literature.

which leads to the **Fornberg Whitham equation**[4] ([7],[6]),

$$u_t + uu_x + (1-\partial_x^2)^{-1}u_x = 0 \tag{3.5}$$

which we will discuss in the following.

Alternative Representations

As mentioned in the introduction, there are several common alternative representations of (1.1). The most common is (3.5) from which one quickly models

$$u_t + uu_x = -v \tag{3.6}$$

$$v - v_{xx} = u_x. \tag{3.7}$$

What our numerical solver is also based on. [5] preferred the following in his analysis,

$$\begin{aligned} u_t + uu_x &= v_x \\ v - v_{xx} &= u. \end{aligned} \tag{3.8}$$

and motivated it via a two-species-Euler-Poisson-system (see [5]). They also analysed this system numerically. We stick for our numerical algorithm to the representation method introduced in [8].

3.2 Analytical results

In this section we primarily quote some theorems from [9] and [8]. The first is a special case from [9]:

Theorem 6 *([9], Theorem 1[5])*
Let $u_0 \in H^2$, then there exists a lifetime $T > 0$ and a unique solution $u \in C([0;T]); H^2)$ of the initial value problem (1.2), which depends continuously on the initial data. Additionally, we have the solution size and minimum lifespan estimates

$$\|u(t)\|_{H^2} \leq 2\|u_0\|_{H^2}, \text{ for } 0 \leq t \leq T \leq \frac{c}{2\|u_0\|_{H^2}},$$

where c is a positive constant.

As mentioned in the introduction, numerically we consider the Fornberg Whitham equation with periodic initial data. Analogously, citehoermann considers the FWE on

[4] As stated in the just mentioned article, we would like to note here that a Taylor expansion of the wave velocity c results in $1 - k^2 + O(k^4)$, where $1 - k^2$ was the wave velocity of the Korteweg-de Vries equation "with an additional term u_x normalized out"([6], 1978, page 385). Therefore, the models for small k are supposed to behave very similarly.

[5] Holmes prooved a more general case for $u_0 \in H^s$, $s \geq \frac{3}{2}$ with c depending on s.

the torus $\mathbb{T}$ so from here on only periodic solutions are considered. For weak entropy solutions we even have a stronger result in [8] then theorem 6:

Theorem 7 *[8], Theorem 2.2*
Let $T > 0$ be arbitrary. For any $u_0 \in L^\infty(\mathbb{T})$, there exists a unique weak entropy solution of the initial value problem (1.2)on the time interval $[0, T]$.

The next one is a statement mentioned in [8]

Lemma 2 *For $u \in L^2(\mathbb{T})$, the function $(1-\partial_x^2)^{-1}u_x$ belongs to $H^1(\mathbb{T})$.*

Proof *We will employ a commonly used method. In the first step we map the $L^2(\mathbb{T})$ to $l^2(\mathbb{Z})$ using the Fourier transform $\mathcal{F}$.*

Then we consider the Fourier transformation of f, f' and f'' to represent the operator $(1-\partial_x)$ and thus also $(1-\partial_x)^{-1}$ in l^2.

If we identify the H^k with a suitable subspace of the l^2, we see that our operator $g = (1-\partial_x)^{-1}$ maps to a subspace that can be identified with the H^{k+2}. Let us start with the technical details.

The Fourier transform is a unitary map with

$$\begin{aligned} \mathcal{F} : L^2(\mathbb{T}) &\to l^2(\mathbb{Z}) \\ f &\mapsto (\hat{f}(n))_{n\in\mathbb{Z}} \end{aligned}$$

where $\hat{f}(n)$ are the Fourier coefficients given by

$$\hat{f}(n) = \int_0^1 \exp(-2\pi i n x) f(x) dx.$$

For $f \in C^1(\mathbb{T})$ we then have

$$\hat{f'}(n) = \int_0^1 \exp(-2\pi i n x) f'(x) dx = 2\pi i n \hat{f}(n)$$

after using integration by parts and the periodicity of f. Analogously we get for $f \in C^2(\mathbb{T})$

$$\hat{f''}(n) = -4\pi^2 n^2 \hat{f}(n)$$

and thus

$$[(1-\partial_x)^2 f]\,\hat{}\,(n) = (1+4\pi^2 n^2)\hat{f}(n).$$

We then have for our operator

$$[(1-\partial_x)^{-1} f]\,\hat{}\,(n) = \frac{\hat{f}(n)}{1+4\pi^2 n^2} =: M\hat{f}(n).$$

Now we identify the $H^k(\mathbb{T})$ for $k \in \mathbb{N}_0$ as a subspace of $L^2(\mathbb{T})$ fulfilling the property

$$H^k(\mathbb{T}) = \{f \in L^2(\mathbb{T}) | ((1 + 4\pi^2 n^2)^{\frac{k}{2}} \hat{f}(n))_{n\in\mathbb{Z}} \in l^2(\mathbb{Z})\}.$$

To match this we define

$$l_k^2(\mathbb{Z} := \{(a(n))_{n\in\mathbb{Z}} \in l^2(\mathbb{Z}) | ((1 + 4\pi^2 n^2)^{\frac{k}{2}} a(n))_{n\in\mathbb{Z}} \in l^2(\mathbb{Z})\}.$$

Then we see that for our operator g the following applies

$$g = \mathcal{F}^{-1} \circ M \circ \mathcal{F}$$

or more in detail

$$\begin{tikzcd} l_k^2 \arrow[r, "M"] & l_{k+2}^2 \arrow[d, "\mathcal{F}^{-1}"] \\ H^k \arrow[u, "\mathcal{F}"] \arrow[r, "g"'] & H^{k+2} \end{tikzcd}$$

which ends the proof. □

These results have important implications for our further deliberations. First of all, we would like to point out that when $u \in L^2(\mathbb{T})$, the function $v = (1 - \partial_x^2)^{-1} u_x$ is a function on the torus $\mathbb{T}$ too. Therefore we have to consider our function v in the numerical scheme with periodic boundary conditions. Furthermore the term $(1 - \partial_x^2)^{-1} u_x$ does not change our Rankine Huginot condition.

Corrolar 1 *The term $(1 - \partial_x^2)^{-1} u_x$ belongs to $H^1(\mathbb{T})$ for $u \in L^2(\mathbb{T})$ since the operator T. Thus it has no influence on the propagation speed of a shock defined by the Rankine-Huginot jump relation.*

Proof *The first half is a corrolar of the previous lemma 2 in combination with the fact that $H^1(\mathbb{T})$ is continuous embedded in $C(\mathbb{T})$. Additionally it is of the form $g \in B(H^k, H^{k+1})$ as in theorem 3.* □

Why do we need the last corrolar? In our Godunov scheme, we chose our CFL condition so that solutions do not intersect, or if they do, only in one cell. For this we needed the speed of the shock. We now know, if we apply the Godunov scheme to our Fornberg Whitham equation, we can use the same CFL condition as in the Burgers equation.

3.3 The numerical discretization

Recall that due to the non-linear in the first equation of (1.2) we use FVM to calculate our approximate solution u_j^n in (3.6) as cell averages of the form (2.25). The second equation (3.7) is linear with a diffusion term v_{xx}. Therefore [5] and [8] suggest a finite difference scheme where v_j^n approximates our solution $v(j\Delta x, n\Delta t)$. In the following we briefly outline our numerical scheme in pseudocode.

1. At the beginning we initialize u^0 via $u_i^0 = \frac{1}{\Delta x}\int_{x_i-1/2}^{x_i+1/2} u_0(x)dx$
2. Calculate v^0 by using u^0 and discretizing the second equation in (1.2) with a central difference scheme
3. For $n = 0, \dots, T$,
   a) Calculate $u^\star(u_j^n, u_{j+1}^n)$ and $u^\star(u_{j-1}^n, u_j^n)$ using the Godunov scheme (2.26)
   b) Calculate u^{n+1} via
   $$u_j^{n+1} = u_j^n - \frac{\Delta t}{\Delta x}(f(u^\star(u_j^n, u_{j+1}^n)) - f(u^\star(u_{j-1}^n, u_j^n))) - \Delta t \cdot v^n$$
   c) Calculate v^{n+1} analogue to 2.

Some remarks, we assume u is periodic and thus $u_0^n = u_N^n$ for all n. The values v_k^n can be calculated using the following discretization

$$v_k^n - \frac{v_{k+1}^n - 2v_k^n + v_{k-1}^n}{\Delta x^2} = \frac{u_{k+1}^n - u_{k-1}^n}{2\Delta x},$$

or to be more specific, by solving the linear equation system $Av = \tilde{u}$ with

$$A = \begin{pmatrix} 1+2\Delta x^{-2} & -\Delta x^{-2} & 0 & \dots & 0 & -\Delta x^{-2} & 0 \\ -\Delta x^{-2} & 1+2\Delta x^{-2} & -\Delta x^{-2} & \dots & 0 & 0 & 0 \\ \vdots & \vdots & \vdots & \vdots & \vdots & \vdots & \vdots \\ 0 & 0 & 0 & \dots & -\Delta x^{-2} & 1+2\Delta x^{-2} & -\Delta x^{-2} \\ 0 & -\Delta x^{-2} & 0 & \dots & 0 & -x^{-2} & 1+2\Delta x^{-2} \end{pmatrix},$$

$$\tilde{u} = \begin{pmatrix} \frac{u_1 - u_{N-1}}{2\Delta x} \\ \frac{u_2 - u_0}{2\Delta x} \\ \vdots \\ \frac{u_N - u_{N-2}}{2\Delta x} \\ \frac{u_1 - u_{N-1}}{2\Delta x} \end{pmatrix}$$

where we assume periodic boundary conditions. Note that only the right hand side $\tilde{u}$ has to be calculated in every time step only, that for A^{-1}, a sparse matrix, does not.

As mentioned previously in corollar (1) the speed of the shock does not change compared to Burgers equation. Thus we can keep the same CFL condition

$$|\frac{\Delta t}{\Delta x} f(u_j)| \leq \frac{1}{2}.$$

Since boundedness of $f(u_j)$ by $f(u_0)$ is not guaranteed - the only result available is theorem 6 - we choose, similar to [8] a safety factor.

3.4 Numerical experiments

In their concluding remarks in [8] stated four questions, which we would like to quote briefly here:

(i) Existence of periodic traveling waves with jump discontinuities (i.e, non-decreasing shocks), although the case of a single jump could be ruled out.

(ii) Boundedness of the spatial minimum and maximum of $u(t)$ as a function of t and independent of the existence time T.

(iii) Wave breaking in more generic cases than those covered by the asymmetry condition in the wave breaking theorems.

(iv) Global (in time) existence of strong solutions for (generic) initial data with small Sobolev norm.

Furthermore, in section 3.1 they ask the question of the lifetime of the classical solution depends on the amplitude q in $u(x, 0) = q\cos(2\pi x)$. This fits in content to question (iv). Due our numerical experiments question (iv) extend to (v): "Does a critical time T exist, depending on the Sobolev norm, after that the solution exists for all time". Another question (vi) is added. If and if yes, how fast does the function v converges towards 0. This could be an explanation of many typical phenomena of the burgers equation and a fast decay to 0 was observed in multiple experiments.

3.4.1 Heuristic approaches

If we examine the lifetime of our solution, we can heuristically reduce the appearance of a shock to two cases by using the Godunov scheme.

We will call these two cases shocks of type 1 and type 2. Type 2 shocks can occur when two parts of the wave move towards each other. In the Burgers equation, for example, this occurs when our solution is positive to the left of a zero and negative to the right. Type 1 shocks can occur when the upper part of a wave is faster than the lower part.

This motivates us to choose our initial conditions as explained in the following.

3.4.2 The initial data and the mesh size

We focus on three types of initial data. We begin with non continuous initial conditions since Hörmann and Okamoto ask in (i) for travelling waves that have more than one discontinuity.

We analyse again, like [8] functions of the form $q\cos(2\pi x)$, whereby we also investigate a faster frequency, thus our initial data has the form $q\cos(2n\pi x)$, $n \in \mathbb{N}$. On this basis, we also consider functions of the form $q\cos(2n\pi x) + b$.

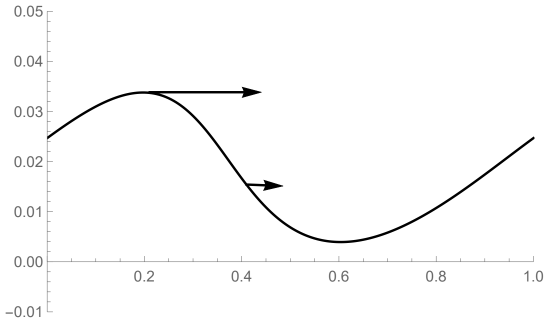

(a) A shock of type 1.

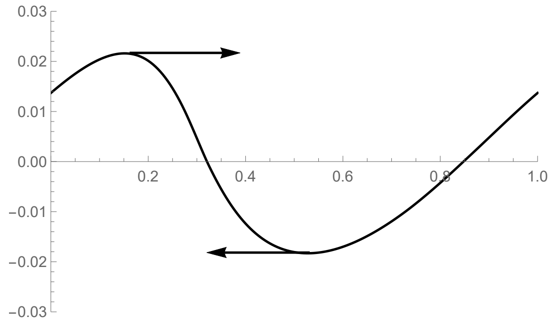

(b) A shock of type 2.

Figure 3.1: On the left the top overtakes the bellow parts, on the right, top and bottom drive towards each other.

All graphics, if not stated differently, were performed with a net size of $\Delta x = 200$ and $\Delta t = 800$. Thus, the CFL condition for our input data was always fulfilled. To make sure that the mesh is fine enough, runs with a finer step size, more precisely $\Delta x = 800$ and $\Delta t = 3200$, were performed at the beginning. We see in the following figures 3.2 and 3.3 two examples that the step size makes no difference, except that in the latter example the shock has a clearer edge.

3.4.3 H^2-norm of $q\cos(2\pi nx) + b$

Most numerical experiments are carried out on functions of the above form. Due to the result in theorem 6 we now calculate the H^2 norm for these functions

$$\|q\cos(2\pi nx) + b\|_{H^2}^2 = q^2\left(8\pi^4 n^4 + 2\pi^2 n^2 + \frac{1}{2}\right) + b^2. \tag{3.9}$$

We see that the frequency, depending on n, according to [9] should have a stronger influence on the life span of a classical solution, as the amplitude q or the offset b. Additionally, a small q can compensate a large n and vice versa. The factor b has a shortening effect for the guaranteed life span which won't occur in our experiments.

3.4.4 Non-continuous initial data

Hörmann and Okamoto have already ruled out the case of a travelling wave with a single discontinuity in [8]. We therefore tested functions u_0 with several shocks, explicitly also initial conditions with only positive values. In all cases examined, the non-continuous initial conditions converge against a continuous function. In figure (3.4) we have as initial condition

$$u_0(x) = \begin{cases} 0.015(x - 0.25), & x < 0.5 \\ 0.015(x - 0.75), & x \geq 0.5 \end{cases}.$$

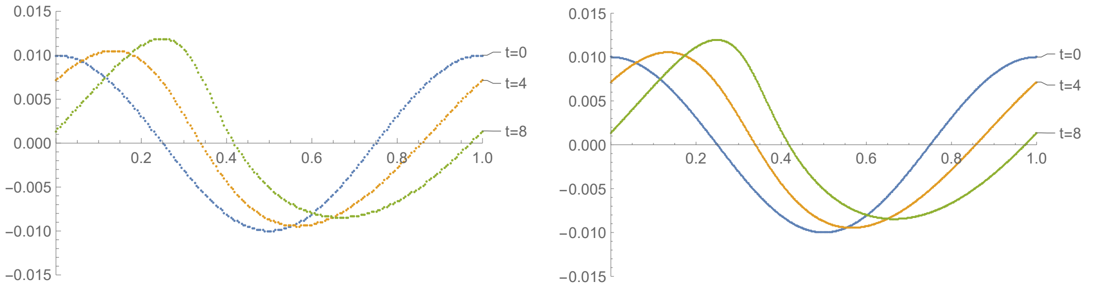

Figure 3.2: On the left, $\Delta x = 200$ and $\Delta t = 800$, on the right $\Delta x = 800$ and $\Delta t = 3200$, both for $u_0(x) = 0.01\cos(2\pi x)$.

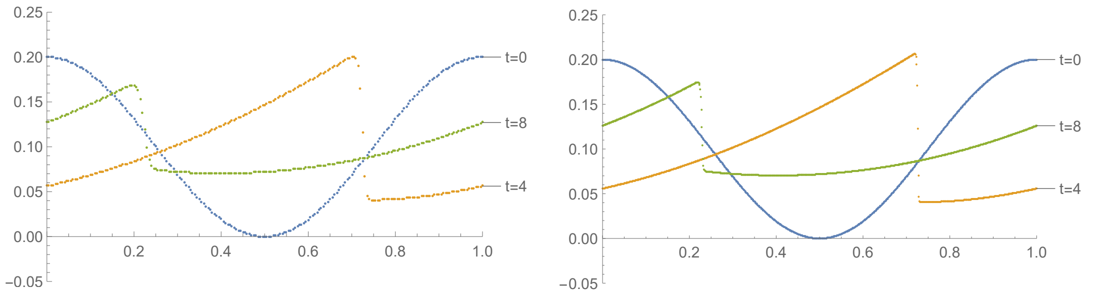

Figure 3.3: The same mesh sizes as above in figure 3.2, this time for $u_0(x) = 0.01\cos(2\pi x) + 0.01$. Here the occurring shock has for $\Delta x = 800$ a clearer edge.

3.4.5 Similarities to the Burgers equation

As just mentioned at the beginning of (3.4), a rapid decay of v to 0 could cause the Fornberg Whitham equation to possess typical phenomena of the Burgers equation. If one considers in the following the exact periodic solutions of the equation

$$\begin{aligned} v - v_{xx} &= u_x \\ u(x) &= q\cos(2\pi n x), \end{aligned}$$

$n \in \mathbb{N}$ and $q = 0.008$. In [8], the authors assume for $q < 0.01$ an infinite lifespan for $q\cos(2\pi x)$. We get a similar result as can be seen in figure 3.5.

However, if we increase the frequency via n, we see that the amplitude of the analytical solution v drops sharply. We can see in figure 3.6 the plots of the exact solutions v_0 for given u_0 with $q = 0.008$.

Analogue the numerical solution of our Fornberg Whitham equation behaves more and more similar to the typical N-waves of the Burgers equation as can be seen in figure 3.7.

In the following we visualize the L^2 norm for v in the first five seconds. We calculated

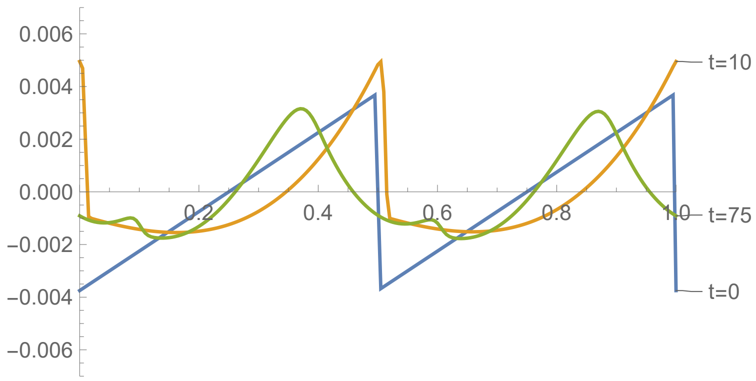

Figure 3.4: The non-continuous initial data converges against a continuous solution

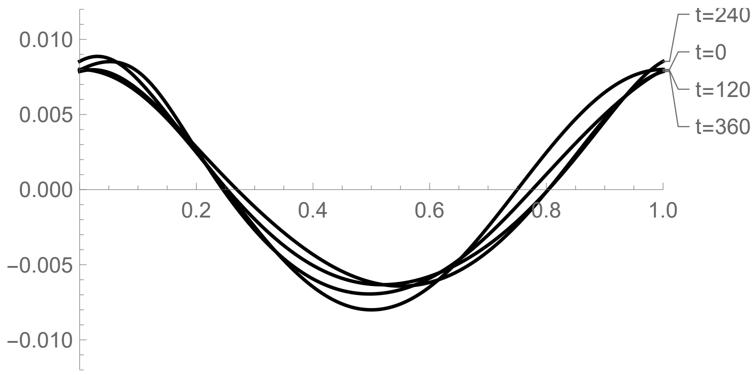

Figure 3.5: $0.008\cos(2\pi x)$ shows some diffusion in $t \in [0, 360]$

the L^2-norm via the discrete formulation

$$\|v^t\|_{L^2}^2 = \sum_{j=0}^{N} (v_j^t)^2 \Delta x.$$

We see in figure 3.8 that apparently a shift b also influences v additionally to an increase of n which has an decreasing effect on v:

In our calculation the factor b has no influence on v^0 since the derivative in u_x. Therefore the decrease of the norm for the same amplitude q must be dependent on the frequency and thus on n. In figure 3.8 (b) the L^2 norm of v decreases exponentially, whereas in (a) it only decreases for a high frequency. In both cases our initial data has the same amplitude $q = 0.01$. Thus we can assume that $b = 2$ is the reason. Figure (c) looks similar to (a). In both cases the N-waves occur for $n \geq 2$ after a short period of time. The function v seems to be from the start $t = 0$ too small in comparison to u to make an influence and thus our solution has similarities to Burgers equation. Figure (d) shows us that a high amplitude also has an decreasing influence on v. The Burgers equation has some properties the Fornberg Whitham equation doesn't have, for example a zero is not

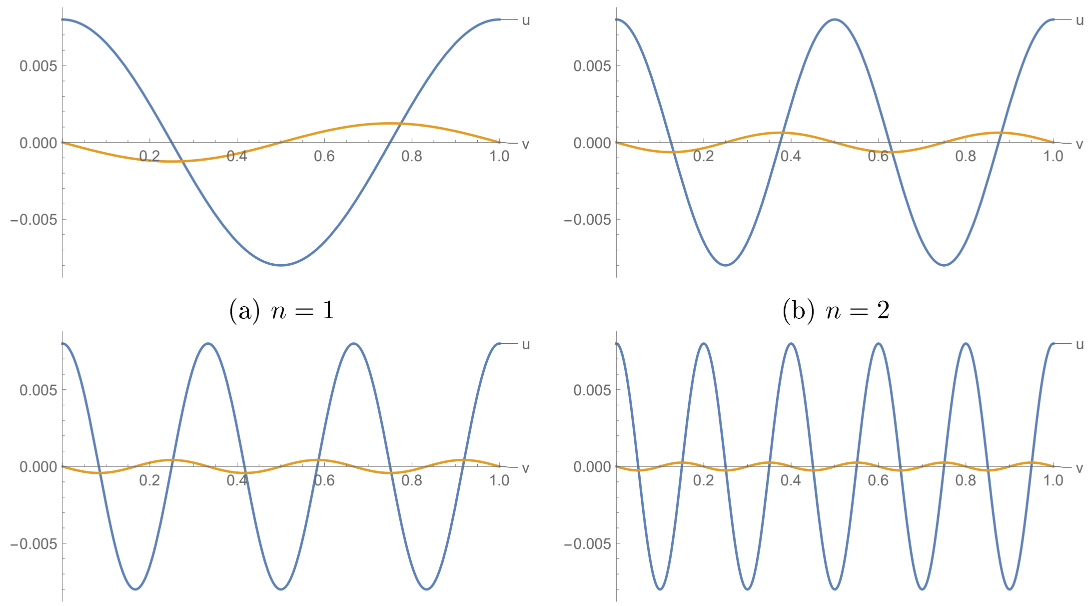

(a) $n = 1$ (b) $n = 2$

(c) $n = 3$ (d) $n = 5$

Figure 3.6: We increase the frequency of $u_0(x) = 0.008\cos(2n\pi x)$ and see, how v_0 tends to 0. Here no numerical approximation was used.

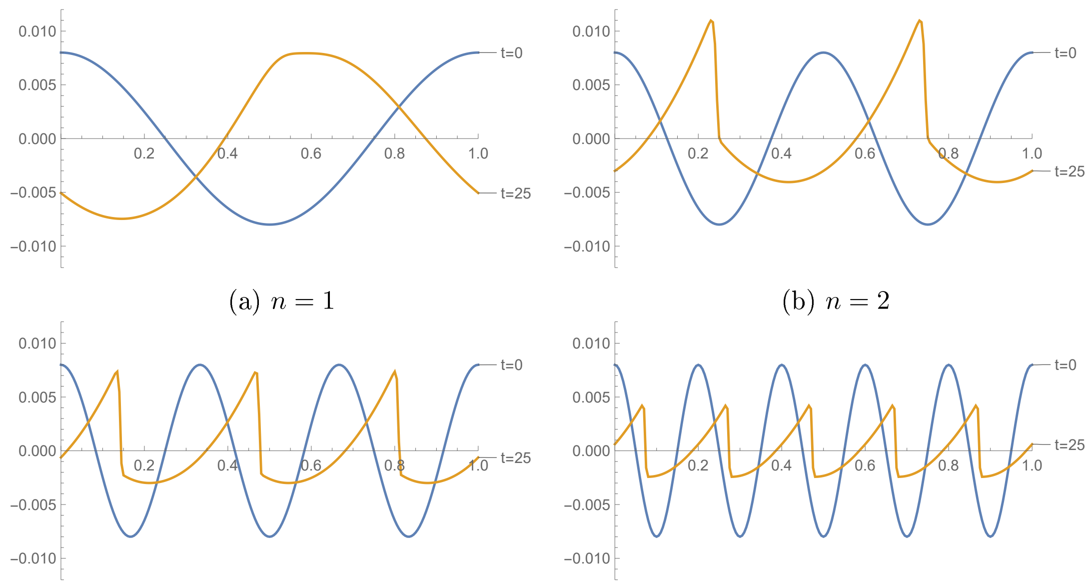

(a) $n = 1$ (b) $n = 2$

(c) $n = 3$ (d) $n = 5$

Figure 3.7: With increasing n the typical N-waves occur with $u_0(x) = 0.008\cos(2n\pi x)$.

travelling but still the similarities suspected on the basis of the investigations on v can

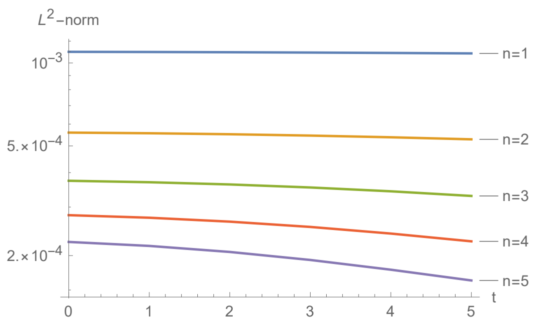

(a) $0.01\cos(2n\pi x) + 0.01$

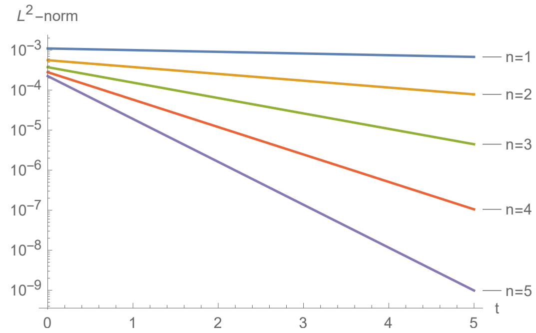

(b) $0.01\cos(2n\pi x) + 2$

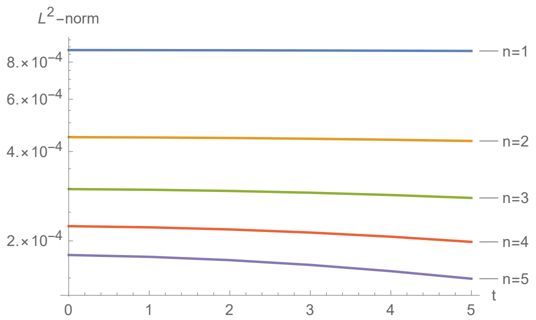

(c) $0.008\cos(2n\pi x)$

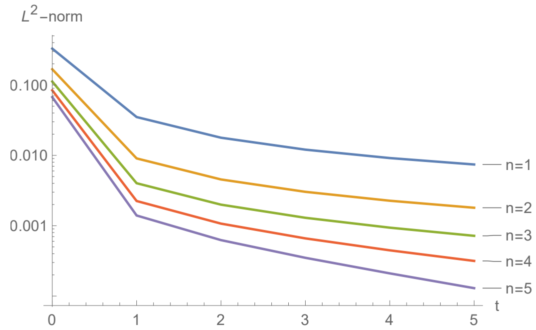

(d) $3\cos(2n\pi x) + 0.2$

Figure 3.8: Different n, b and q.

be clearly seen in the following figure 3.9:

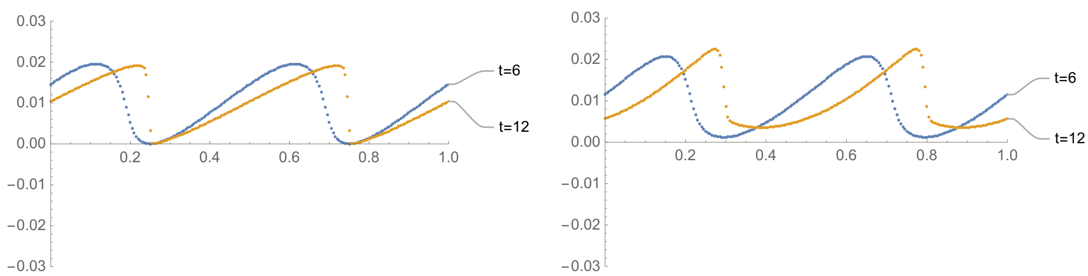

Figure 3.9: On the left the numerical solution of the Burgers equation for $0.1\cos(4\pi x) + 0.1$ next to the corresponding solution of the Fornberg Whitham equation.

3.4.6 Boundedness of the spatial minimum and maximum

As quoted from [9] already, minimum and maximum on the real axis are limited by the H^2 norm. Our numerical experiments do not allow the assumption that $\|u_0\|_\infty$ could be used as a sufficient bound (as also can be seen in figure 3.9), but no case was found where the minimum and maximum exceed $2\|u_0\|_\infty$. Here, however, further numerical and analytical investigations are necessary.

3.4.7 Wave breaking in more generic cases

In general, no asymmetry seems necessary to receive shock waves as assumed in previous papers. The numerical experiments suggest a strong curvature of the initial condition as one possible cause of wave breaking, for our initial condition this results in a high frequency as the origin of the type 2 shocks. This covers with the occurrence of shocks in section (3.4.5) for $q\cos(2n\pi x)$ when the frequency is increased. A higher frequency automatically results in a much higher H^2 norm due to the chain rule shown in (3.9) and thus a shorter guaranteed life span.

Before we examine the curvature of our initial condition and the associated second derivative, we consider another phenomenon. Let us consider functions of type $q\cos(2n\pi x)+b$. Interestingly, an increase of b does not automatically result in a shortened lifespan, although the H^2 norm becomes larger. For $q = 0.01$ and $b = 0.01$ our solution for the initial value $q\cos(2\pi x) + b$ seems to exist forever, but for $q\cos(4\pi x) + 0.01$ it already has only finite life span. This matches the results for $q\cos(2\pi nx)$ from section (3.4.5). For $b = 2$ the picture changes. Although our H^2 norm increases, the lifetime is prolonged.

The solution for the initial condition $0.01\cos(2n\pi x) + 2$ seems to live forever for $n = 1, 2, 3, 4, 5$, it's amplitude heavily decreases and so does v.

It is also very interesting that b, due to differentiation, has no influence in the numerical calculation of v^0. Nevertheless, v converges faster against a constant function than for b equals to zero.

In addition, multiple times solutions occurred with constant speed as can be seen in figure 3.11. Due to our mesh size we only found solutions of the form $q\cos(2 \cdot n\pi x) + b$ with $n = 4$.

3.4.8 Relative change as origin of shocks

The previous section shows that the intuitive assumption, strengthened by the H^2-norm, that the curvature is mainly responsible for the wave breaking is not enough due to the smoothing effect of b. Another approach is the relative change of the solution in an interval. The relative change of a function f is defined by

$$\frac{f(b) - f(a)}{f(a)}.$$

For our initial condition $q\cos(2\pi nx) + b$ we examine the relative change on one of the points with the strongest curvature, $x = 0$. Now the relative change in the interval$[0, \Delta x]$ is given by

$$\frac{u(\Delta x) - f(0)}{f(0)} = \frac{q\cos(2\pi n\Delta x) - q}{q + b}.$$

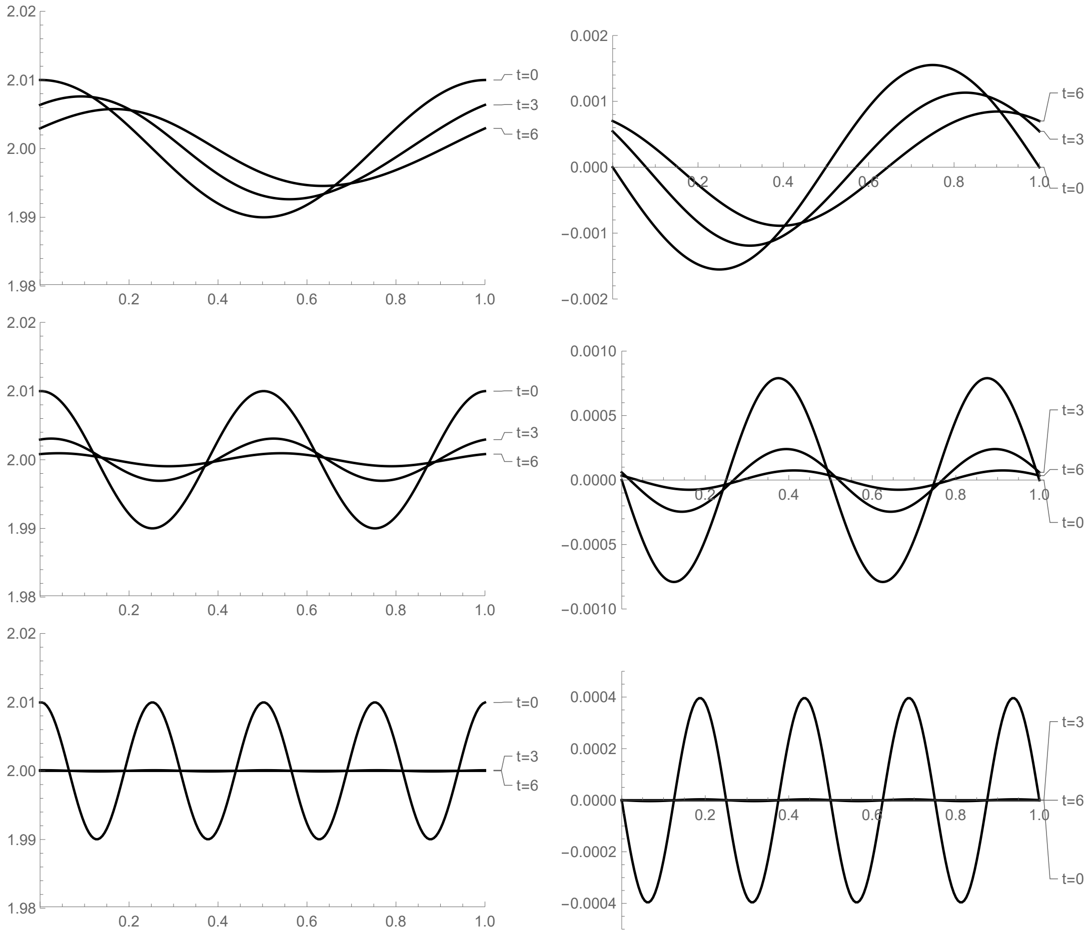

Figure 3.10: On the left u with $u_0(x) = 0.01\cos(2n\pi x) + 2$, on the right v, for $n = 1, 2, 4$. Both tend to 0 with increasing n.

A taylor expansion of degree two gives us

$$-\frac{2qn^2\pi^2(\Delta x)^2}{q+b} + O(x^3)$$

and we see the dependence of q, n and b with n and b having a stronger influence then q. If, as in [9], one assumes an indirectly proportional relationship, then b now extends the lifetime of the classical solution as we have seen in section 3.4.7.

3.4.9 Global (in time) existence of strong solutions

Our numerical experiments give the assumption that wave breaking occurs after a short period of time. In contrast to the Burgers equation, for example, we have mainly determined type 2 shocks. Of course, the definition remains heuristic.

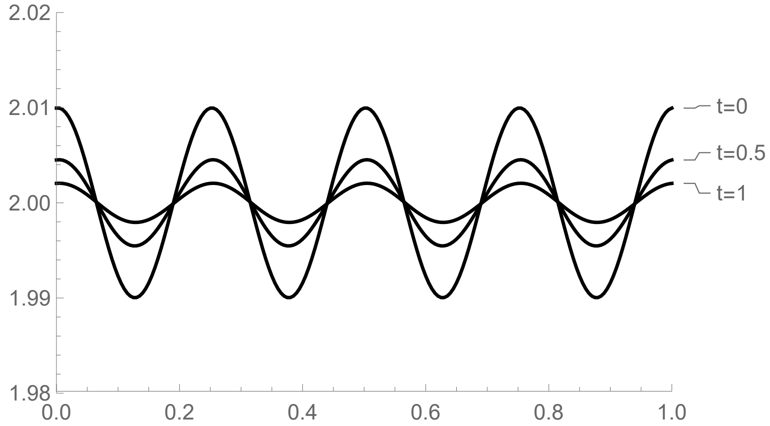

Figure 3.11: The solution for $u_0(x) = 0.01\cos(8\pi x)$ travels with constant speed

This observation coincides with our previous assumptions in section 3.4.8. As the amplitude of the solutions decreases due to the diffusion, the relative change of the function also decreases. If the strong solution survives the assumed critical time interval, the diffusion of the Fornberg Whitham equation seems to outweigh the nonlinear term and infinite lifespan seems to occur. In addition, both as well, occurring shocks and discontinuous initial data, converge against continuous functions after a certain time.

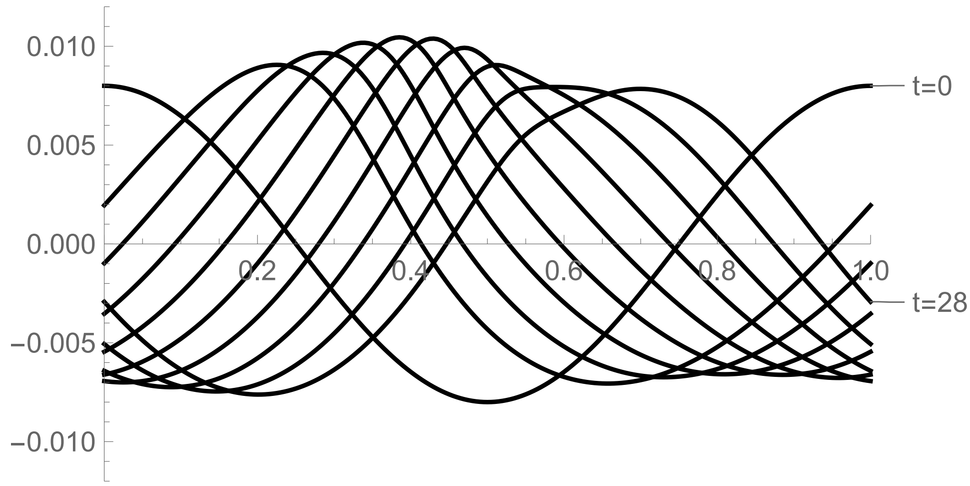

Figure 3.12: $0.008\cos(2\pi x)$ during the assumed critical time period

4 Summary and outlook

4.1 Results

We summarize once again the findings from the numerical experiments.

4.1.1 Travelling waves with a constant speed

An interesting discovery is the occurrence of travelling waves with constant speed. Due to our numerical scheme these were discovered only for period 8π, but for different values of q and b. Thus the speed seems to be dependent only on the frequency. An interesting question is therefore whether this phenomenon also occurs for other frequencies.

In addition, the question arises whether there are non continuous travelling solutions with constant speed. If this were the case, it is more likely that they exist for all time and do not converge against a smooth function.

4.1.2 $v - v_{xx} = u_x$

In general, an analysis of the second equation for periodic solutions and the resulting dynamics is of great importance. So far, as far as we know, the behaviour of v has been ignored in previous work. Two different factors for a rapid drop in v could be found. A summand b and an increase of the frequency via n. This must now be analytically confirmed. We were able to show numerically in section 3.4.5 that the similarity to Burgers equation is thus explainable.

4.1.3 Lifespan estimates

The idea of the relative change of smooth periodic functions (as an initial data) for estimating their lifetime should be pursued analytically. The results so far from [9] expect a shortening of the guaranteed life time of a classical solution through an increase in the factor b. In the relative change, this factor, heuristically speaking, leads to an extension of lifetime as we observed numerically.

4.2 Improvements in the code

As already noted in [8], there is potential for improvement especially in solving the second equation in 1.2. The discoveries made in the numerical experiments also underline once again the importance of the second equation. One could for example use the Fast-Fourier-Transformation (FFT) like [5] did. Nevertheless, we would like to point out that they obtained similar results with FFT as well as with the centered difference method. The Godunov method used in the first equation is only of order 1, but it can be used as a basis for higher order methods such as in [1] and [15] chapter 15.6.

5 Appendix

5.1 The numerical scheme

The code used in Mathematica to export the data is given in the following:

```
(*variables used*)
a0 = 0.1;
b0 = 0;
a1 = a0 + b0;
f[x_]:=a0 * Cos[2Pi * x] + b0;
dx = 1/200;
dt = 1/800;
dtend = 10000;
dtexp = 100/4;
c = dt/dx;
xx = Table[x, {x, 0, 1, dx}]//N;
NN = Length[xx];
U = ConstantArray[
0, {2, NN}];
V = ConstantArray[
0, {2, NN}];

(* calculating u_0 und A *)
For[
i = 1, i ≤ NN, i++,
U[[1, i]] = 1/dx * Integrate[f[x], {x, xx[[i]] − 1/2dx, xx[[i]] + 1/2dx}]//N
```

```
];
U[[1,NN]] = U[[1,1]];
AA = SparseArray[
{Band[{1,1}] → 1 + 2dx^(−2),
{1,2} → −dx^(−2),
{1,NN − 1} → −dx^(−2),
{NN,NN − 1} → −dx^(−2),
{NN,2} → −dx^(−2),
Band[{2,3},{NN − 1,NN}] → −dx^(−2),
Band[{2,1},{NN,NN − 1}] → −dx^(−2)},{NN,NN}];
A = LinearSolve[AA];

laufzeit = Timing[
For[
t = 1,t ≤ dtend,t++,
(* v_0 ausrechnen für t*)
bb = {
(U[[1,2]] − U[[1,NN − 1]])/(2dx),
Table[(U[[1,i + 2]] − U[[1,i]])/(2dx),{i,1,NN − 2}],
(U[[1,2]] − U[[1,NN − 1]])/(2dx)
}//Flatten;
V[[1]] = A@bb;


(* the first flux*)
w1 = ConstantArray[
0,NN
];
For[i = 2,i ≤ NN − 1,i++,
```

```
If[
U[[1, i + 1]] ≥ 0&&U[[1, i]] ≥ 0,
w1[[i]] = U[[1, i]],
If[
U[[1, i + 1]] < 0&&U[[1, i]] < 0,
w1[[i]] = U[[1, i + 1]],
If[
U[[1, i + 1]] > 0&&U[[1, i]] < 0,
w1[[i]] = 0,
If[
U[[1, i + 1]] < 0&&U[[1, i]] > 0,
If[
U[[1, i + 1]] + U[[1, i]] < 0,
w1[[i]] = U[[1, i + 1]],
w1[[i]] = U[[1, i]]
]
]
]
]
]
]
(* periodic boundary *)
If[
U[[1, 2]] ≥ 0&&U[[1, 1]] ≥ 0,
w1[[1]] = U[[1, 1]],
If[
U[[1, 2]] < 0&&U[[1, 1]] < 0,
```

```
w1[[1]] = U[[1,2]],
If[
U[[1,2]] > 0&&U[[1,1]] < 0,
w1[[1]] = 0,
If[
U[[1,2]] < 0&&U[[1,1]] > 0,
If[
U[[1,2]] + U[[1,1]] < 0,
w1[[1]] = U[[1,2]],
w1[[1]] = U[[1,1]]
]
]
]
]
];
w1[[NN]] = w1[[1]];
(* the second flux *)
w1;
w2 = Drop[Flatten@{w1[[NN − 1]], w1}, −1];
(*calculateu^{t + 1}*)
U[[2]] = U[[1]] − c ∗ (w1^2/2 − w2^2/2) − dt ∗ V[[1]];
U[[2, NN]] = U[[2, 1]];

(* exporting the data*)
If[Mod[t, dtexp] == 1,
Export[
ToString[t] <> ".mat", U[[2]]];
```

```
];
If[Mod[t, dtexp] == 1,
Export[
V <> ToString[t] <> ".mat", V[[1]]
];
];
Clear[w1, w2];
U[[1]] = U[[2]];
]
]
```

Literaturverzeichnis

[1] J. Bell, P. Colella, and A Trangenstein. Higher order godunov methods for general systems of hyperbolic conservation laws. *Journal of Computational Physics*, 82:362–397, 1989.

[2] M. Crandall and A. Majda. Monotone difference approximations for scalar conservation laws. *MATHEMATICS OF COMPUTATION, VOLUME 34, NUMBER 149*, pages 1–21, 1980.

[3] L. Debnath. *Nonlinear Partial Differential Equations.* Birkhäuser Boston, 2005.

[4] L. Evans. *Partial Differential Equations.* American Mathematical Society, 2010.

[5] K. Fellner and L. Schmeiser. Burgers-poisson: A nonlinear dispersive model equation. *SIAM J. Appl. Math.*, 64:1509–1525, 2004.

[6] B. Fornberg and Whitham F. A numerical and theoretical study of certain nonlinear wave phenomena. *Mathemactial and Physical Sciences*, pages 373–404, 1978.

[7] G. Hoermann. Wave breaking of periodic solutions to the fornberg-whitham equation. *Discrete and continuous Dynamical Systems*, 38:1605–1619, 2017.

[8] G. Hoermann and Okamoto H. Weak periodic solutions and numerical case studies of the fornberg-whitham equation. *arXiv:1807.02320*, 2018.

[9] J. Holmes. Well-posedness of the fornberg–whitham equation on the circle. *J. Differential Equations*, 26:8530–8549, 2016.

[10] W. Hundsdorfer and J. Verwer. *Numerical Solution of Time-Dependent Advection-DiffusionReaction Equations.* Springer-Verlag, 2003.

[11] A. Jüngel. Modeling and numerical approximation of tra±c flow problems. Lecture Notes, 2002.

[12] A. Jüngel. Partielle differentialgleichungen. Lecture Notes, 2017.

[13] J. Levandosky. Math 220a lecture notes. Lecture Notes, 2002.

[14] R. LeVeque. *Numerical Methods for Conservation Laws.* Springer Basel AG, 1990.

[15] R. LeVeque. *Finite Volume Methods for Hyperbolic Problems.* Cambridge Texts in Applied Mathematics, 2004.

[16] S. Mishra. Numerical methods for conservation laws and related equations. Lecture Notes.

[17] J. Thomas. *Numerical Parital Differential Equation, Finite Difference Methods.* Springer-Verlag Neq York, 1995.

[18] J. Thomas. *Numerical Parital Differential Equation, Conservation Laws and Elliptic Equations.* Springer-Verlag Neq York, 1999.

[19] S. Ǩruzkov. First order quasilinear equations in several independent variables. *Math. USSR Sbornik*, 10:217–243, 1970.

[20] Ž. Přnic. Godunov scheme for the scalar nonlinear conservation laws with flux depending on the space variable. *Mathl. Comput. Modelling*, 22:1–15, 1995.

[21] F. Whitham. Variational methods and applications to water waves. *The Royal Society Publishing*, 299:6–25, 1967.

[22] G. Whitham. *Linear and nonlinear waves.* John Wiley and Sons, 1974.

[23] L. Williams. Symmetry. Web page, url=https://www.cs.unm.edu/ williams/cs530/, 2011.